

**DESIGN OF A CUBESAT MISSION FOR PERSISTENT SPACE SITUATIONAL
AWARENESS WITH PASSIVE OPTICAL SENSORS**

A Thesis
Presented to
The Academic Faculty

By

Luke James Alexander

In Partial Fulfillment
of the Requirements for the Degree
B.S. in Aerospace Engineering with the Research Option
in the School of Aerospace Engineering

Georgia Institute of Technology

May 2017

Copyright © Luke James Alexander 2017

**DESIGN OF A CUBESAT MISSION FOR PERSISTENT SPACE SITUATIONAL
AWARENESS WITH PASSIVE OPTICAL SENSORS**

Approved by:

Dr. Marcus J. Holzinger
School of Aerospace Engineering
Georgia Institute of Technology

Dr. E. Glenn Lightsey
School of Aerospace Engineering
Georgia Institute of Technology

Dr. Brian C. Gunter
School of Aerospace Engineering
Georgia Institute of Technology

Date Approved: May 1, 2017

If you're the smartest person in the room, you're in the wrong room.

Anonymous

Dedicated to all undergraduates who attempt to build CubeSats.

ACKNOWLEDGEMENTS

I would like to acknowledge Dr. Marcus J. Holzinger for his guidance, support, and mentorship that he has provided throughout my work on this project and throughout my entire undergraduate career. I would also like to acknowledge the staff of the Air Force Research Laboratory Space Vehicles Directorate Small Satellite Portfolio and University Nanosat Program and the countless graduate and undergraduate students that were involved with RECONSO before, during, and after my tenure on the project.

TABLE OF CONTENTS

Acknowledgments	v
List of Tables	viii
List of Figures	x
Chapter 1: Introduction and Background	1
1.1 Literature Review	2
Chapter 2: Methods and Materials	5
2.1 Methods	5
2.2 Materials	8
2.2.1 Payload Hardware Selection	9
Chapter 3: Results	12
3.1 Requirements Design	12
Chapter 4: Discussion	15
4.1 ADCS Trade	15
4.1.1 Objectives of trade	16
4.1.2 Trade evaluation	18
4.1.3 Evaluation of Inertial Measurement Unit	21

4.1.4	Evaluation of GPS Receiver	23
4.1.5	Evaluation of GPS Antenna	25
4.1.6	Evaluation of ADCS Microcontroller	27
4.1.7	Trade Conclusion and Summary	29
4.2	CDH Trade	29
4.2.1	Objectives of trade	30
4.2.2	Trade evaluation	32
4.2.3	Evaluation of Downlink System	39
4.2.4	Evaluation of Ground Station	44
4.2.5	Trade Conclusion and Summary	45
4.3	CONOPS	46
4.3.1	Overview of RECONSO hardware and software	46
4.3.2	Overview of Flight Software	46
4.3.3	Spacecraft Modes of Operation	49
Chapter 5: Conclusion		52
Appendix A: UHF Radiation Pattern		55
Appendix B: Link Budget Analysis		57
Appendix C: Mode Switching Flow Chart		59
References		59

LIST OF TABLES

2.1	Sample COTS Lens components	11
2.2	Sample COTS sensor components	11
3.1	RECONSO Mission Objectives	12
3.2	RECONSO Mission Design Requirements	13
3.3	RECONSO Mission Success Criteria	14
4.1	Initial status of ADCS hardware	15
4.2	Reasoning for opening trade on each component	16
4.3	Dimensions of different sun sensor options	20
4.4	Sun sensor technical specifications	20
4.5	IMU technical specifications	22
4.6	GPS Receiver technical specifications	24
4.7	GPS Receiver decision	25
4.8	ADCS Microcontroller technical specifications	28
4.9	Final trade decisions	29
4.10	Status of COM subsystem before trade	29
4.11	Status of ground station before trade	30
4.12	Aspects of ground station opened for trade along with reasoning	31

4.13	Technical specifications of UHF antenna options	38
4.14	Management risks of UHF antenna options	39
4.15	UHF antenna trade evaluation	39
4.16	NearSpace Launch cost of GlobalStar Duplex operation	43
4.17	All components of RECONSO flight hardware and software.	47
4.18	Operational components of the RECONSO system throughout all modes. . .	51

LIST OF FIGURES

2.1	Observer i and space object j geometry	6
2.2	Visualization of detectable volume	6
2.3	1U and 2U aperture design options for a 6U CubeSat.	10
4.1	NSS CubeSat Sun Sensors	19
4.2	MAI Sun Sensors	19
4.3	In-house brass-board prototype of photodiode sun sensors	19
4.4	Analog Devices ADIS16365	21
4.5	Skyfox Labs piNAV-L1 GPS	23
4.6	Novatel OEM615 GPS	23
4.7	Pumpkin GPSRM 1 GPS Receiver	23
4.8	SSBV Space-based GPS Receiver	23
4.9	AntCom 1.5G15A-18NM-1-S	26
4.10	Skyfox PocketQube GPS Patch Antenna	26
4.11	Skyfox Space-Friendly CubeSat GPS Antenna	26
4.12	Spacecraft structure and packaging of RECONSO	27
4.13	ISIS Quad monopole turnstile antenna on 2U face opposite the payload.	33
4.14	Radiation pattern of the ISIS Monopole antenna on a 2U CubeSat contoured from -20 dBi to 0 dBi	34

4.15	Radiation pattern of the ISIS Monopole antenna on a 3U CubeSat bus contoured from -20 dBi to 0 dBi.	34
4.16	Depiction of the stowed GOMspace AT430 antenna mounted on the 2U face opposite the optical train.	35
4.17	Depiction of the deployed GOMspace AT430 antenna mounted on the 2U face opposite the optical train.	36
4.18	Radiation pattern of the GOMspace AT430 antenna contoured from -0.8 dBi to 4 dBi. This option exhibits higher gain and higher directionality than the ISIS option.	36
4.19	A mounting apparatus typical of a tape measure UHF antenna.	37
4.20	The tape measure antenna shown on the flight-ready Finnish Aalto-1 satellite.	37
4.21	Availability for placement of S-Band patch antenna on structure.	41
4.22	Placement of the GlobalStar Duplex board integrated with the satellite internals. The GlobalStar board and patch antenna are emphasized with arrows.	42
4.23	Wiring documentation of the Duplex MODEM Suite and Tyvak Intrepid.	42
4.24	Summary of Uplink/Downlink systems through primary and secondary channels	44
4.25	Operation of RECONSO over the course of the entire mission lifetime.	49
4.26	Operation of RECONSO over the course of a given orbit.	50
A.1	Mock-up of the RECONSO 6U structure	55
A.2	Resultant radiation pattern on UHF for the ISIS Dipole antenna	55
B.1	UHF gain calculated at various orbital altitudes	57
C.1	Flight software CONOPS flow chart	59

SUMMARY

This paper will explore the design and implementation of a CubeSat with an electro-optical sensor for purposes of space situational awareness. The Introduction gives an overview of the current state-of-the-art for space-based space object detection. It is clear that the next step in space mission design for space situational awareness is the application of optical detection to the CubeSat form factor. The Methods and Materials section covers the abstract design parameters and theoretical concept of operations of a spacecraft that has the goal of detecting as many space objects as possible before exploring how hardware can be selected to best meet the goals of the science objective. The Results section discusses the requirements that were flowed down from this theoretical study to guide the development of a CubeSat to fulfill this mission profile. The Discussion then goes through the hardware selection process for every supporting flight system and treats trade studies for all major flight systems as guided by the system requirements, discussing tradeoffs and decisions that were made at all steps of the hardware selection and software design processes. An experimental concept of operations of the satellite is then proposed given the constraints that the selected hardware and operational parameters impose on the system. The Conclusion section gives an overview for the progress that has been made towards this design at the Georgia Institute of Technology with the Reconnaissance of Space Objects CubeSat and explains the next steps for this flight project with a development timeline to launch. Information on specific technical efforts can be found in the Appendix.

CHAPTER 1 INTRODUCTION AND BACKGROUND

The continued and effective use of Earth orbit for all purposes, both commercial and governmental, requires a low Earth orbit (LEO) environment that can be accurately characterized. The growth of space debris over recent years has made such characterization difficult. Fragmentations of rocket bodies, active satellites, and defunct satellites, among other things, have created huge numbers of space objects (SOs) that are very difficult to track [56].

The majority of data on SOs comes from the US Department of Defense Joint Space Operations Center (JSpOC). This data is gathered through the Space Surveillance Network (SSN) that JSpOC tasks with the observation and tracking of SOs. The SSN consists of a network of approximately 30 ground- and space-based sensors that detect and track objects in Earth orbit [5]. Data from the SSN for all non-classified objects is then made publicly available in the form of two line elements (TLEs) via Space-track.org. There are currently in excess of 21,000 LEO objects with diameters above 10 cm [45] in the JSpOC space object catalog (SOC). The TLEs for approximately 16,308 of these objects are publicly available via Space-track.org ¹. The largest contributions to the SSN are ground-based systems that use either visible light or radar [33]. For radar based systems, which are by far the largest contributors to the SSN, Rayleigh scattering makes debris smaller than 10 cm in diameter very difficult to reliably track [15]. As such, the number of objects in LEO below 10 cm can only be estimated. Current estimates place the number of objects larger than 1 cm at approximately 700,000 and the number of objects larger than 1 mm at approximately 200 million [2]. A quick analysis of JSpOC numbers on functional vs. nonfunctional Earth satellites reveals that only around 7% of SOs are operational assets; in essence, 93% of the objects in orbit about Earth serve to do nothing other than limit and endanger on-orbit assets [31].

The situation continues to worsen at a concerning rate. Events such as the 2007 Anti-Satellite (ASAT) test on the defunct Fengyun-3 weather satellite [22] and the 2009 collision between the defunct Cosmos-2251 and the operational Iridium-33 [54] have both significantly worsened the situation. These two events alone doubled the number of space objects larger than 1 cm, producing over 250,000 new pieces [23]. Continuing ASAT tests [34] will only lead to a further deterioration of the situation. Orbital debris larger than 10 cm in diameter can cause catastrophic failure in most space missions, and debris in the 1 to 10 cm regime can easily disable or damage core mission functionality [19]. Damage from debris in the 1 to 10 cm regime has posed a catastrophic risk to the Space Shuttle on multiple occasions [46, 6]. It has been established that the cascading collisions of debris at a critical density has the potential to render Earth orbit inaccessible [24], and action must be taken to accurately assess the situation before it becomes untenable.

There is currently action being taken via many different avenues. Space situational awareness (SSA), the characterization of the space environment, has been listed as a pri-

¹via www.space-track.org; accessed 3/30/2017

ority for research and technology advancement at many levels of the United States government. The Presidential Space Policy under the administration of U.S. President Barack Obama calls for increased knowledge of the space environment [35]. The Presidential Space Policy has informed the policy of the Joint Chiefs of Staff in Joint Publication 3-14, which recognizes increased SSA as one of the most important areas for increased research and new technology in the coming decade [41, 51]. As a result, the recent FY2016 US Defense Budget Request includes increases in funding to the Space Based Space Surveillance (SBSS) mission and the JSpOC Mission System (JMS) [18]. Recognizing the issue on a global scale, the United Nations Committee on the Peaceful Uses of Outer Space also promotes international cooperation on SSA as it is an issue that affects all space-faring nations [40].

Given the worsening problem in LEO and the clear need for increased SSA, especially regarding objects with diameters from 1 to 10 cm, it is evident that much work remains to be done regarding SO detection. Due to their recent proliferation, opportunities exist in the application of small satellite design paradigms to SO detection.

1.1 Literature Review

Debris detection was first performed with ground-based radars, and radar systems continue to be used for this purpose. Ground-based approaches can be divided into optical imaging and radar imaging. Typically, optical imaging performs much better for objects in geosynchronous Earth orbit (GEO) while radar is better for the observation of objects in LEO [39]. The earliest attempt at SO detection was the radar detection of Sputnik with the Millstone radar at MIT Lincoln Laboratory's Millstone Hill observatory [16]. Very accurate radar observations of small diameter SOs are still made at this site with the MIT Lincoln Laboratory Haystack radar [11] being one of the first dedicated contributors to the SSN. One of the most recent ground-based radar contributors to the SSN is the Space-Fence radar array, which is designed to make approximately 1,500,000 observations of LEO objects each day [33]. Detections of debris smaller than 10 cm have been made with ground-based radar [53, 17], but such observations cannot be made accurately and consistently enough to contribute to the JSpOC SOC. Deep space radar observatories on the Kwajalein atoll have also been successful in the accurate tracking of GEO objects [16].

Ground-based optical approaches for debris detection have been increasingly employed. The most notable of these approaches have been the Optical Ground Station (OGS) [10] and, more recently, the Space Surveillance Telescope (SST) [32]. Both observatories have made substantial contributions to the characterization of the GEO debris environment. Other ground-based optical approaches have involved the repurposing of astronomical telescopes for the observation of LEO debris. Notable examples of this can be found in [27, 55, 3, 38] as summarized by Shell in [44]. However, given that ground-based optical observatories are most effectively applied to GEO observations, their limitation lies in the fact that they are only able to characterize a small portion of the GEO debris belt that is visible from their fixed location. While their observations can be extrapolated to estimate numbers of GEO debris, they cannot be used to actively catalog it.

Space-based systems offer different design paradigms than ground-based systems because of their relative proximity to SOs. One such advantage is the ability to physically

detect the impact of small debris and thus measure its presence. The first approaches in this manner include the PIE experiment on MIR [28] and evidence of debris impact on the space shuttle [6]. An exhaustive review of impact-related in-situ detection is presented by Bauer in [2]. By nature, such experiments are unable to catalog debris that is still in orbit and therefore can contribute only to statistical models of the debris environment rather than track orbits of objects for the SOC.

Space-based radar has not traditionally been applied due to the fact that the use of radar detection requires large structures and high power, both of which make its application exceedingly difficult in a space environment. There are few examples of space-based radar detection of orbital debris in the literature [13].

The application of space-based optical imaging systems to on-orbit debris detection has been very successful. The earliest such mission, the Midcourse Space Experiment (MSX) Space Based Visible (SBV) detector [14] demonstrated effective maturation of the technology necessary for such a mission, and serves as a design standard for space based optical detection mission architectures. The Sapphire mission [29], Space-based Telescopes for Actionable Refinement of Ephemeris (STARE) mission [48] and SBSS mission [52] not only use optical sensors to make on-orbit detections of space debris, but also do so with a similar concept of operations (CONOPS) as the MSX/SBV mission. The MSX/SBV mission proved the design paradigm of placing a sensor in LEO and alternating the data collection of LEO and GEO objects with the data processing of the same objects for down-link to the ground [43]. The Sapphire, STARE, and SBSS missions all do the same. The MSX/SBV, Sapphire, and SBSS missions are also all capable of both tasked and passive observation of SOs. However, all three of these missions are much larger than the STARE mission. The STARE mission, a 3U CubeSat, is the first and only current application of the CubeSat form factor to SO detection. However, even though it is much smaller than similar missions, a review of its optical payload [47] and CONOPS [37] reveals few differences in effectiveness or application.

In fact, CubeSats offer much more potential than other mission architectures for the detection of SOs as their low cost and ease of scalability allows them to be added to a constellation more easily and to adapt to changes in technology more quickly [26]. A constellation is also much more resistant to faults as it is fractionated and disaggregated; a failure of one unit does not result in the failure of the entire system. Planet Labs has recently begun the deployment of a ground-observing CubeSat constellation in LEO [4]. Similar constellation architectures could be adapted for SSA.

A disaggregated system offers many benefits for system redundancy and efficacy [9], but a disaggregated design paradigm has only recently begun to be employed. The SBSS mission is planned to scale to a constellation of satellites, but has yet to be fully deployed. Likewise, Space Fence, one of the most recent approaches to ground-based radar detection, consists of two ground-based radar arrays, but is not planned to scale any further [33]. In short, while many mission architectures do exist to characterize the current situation of debris in Earth orbit, few mission architectures effectively do so in a disaggregated and easily scalable manner.

A constellation may be optimized for debris detection, and a genetic algorithm is well-suited to this problem. Many constellation optimization problems have been addressed using genetic algorithms [8, 12, 30, 25]. As such, the use of such applicable methodology

for optimizing a system of debris observing satellites is well established. Additionally, the use of a constellation allows for the standardization of data processing and can streamline the contributions of a system to the SSN [21].

CHAPTER 2 METHODS AND MATERIALS

Persistent SSA is not only possible using CubeSat technologies, it is the next step in lowering the cost and increasing the quality of relevant SSA information. The CubeSat standards defined by the California Polytechnic State University [36] are used universally by both launch providers as well as CubeSat manufacturers. The recent proliferation of standardized CubeSat technologies has significantly increased the variety and quality of commercially available off-the-shelf (COTS) products ready for use in CubeSat design. The Reconnaissance of Space Objects (RECONSO) CubeSat mission under development at the Georgia Institute of Technology is attempting to launch such a CubeSat in the 2018 timeframe. To begin such a design, all performance and design criteria must be laid out in the abstract. The payload science, CONOPS, and mission profile of a CubeSat for persistent SSA such as RECONSO will be discussed in detail. The methods section will explore first the payload science behind the CubeSat before the materials section explores the hardware selection and trade studies that were outlined for this project.

2.1 Methods

As per system design engineering best practice, the requirements of the system should be defined before the use case for the system can be driven by the limitations of hardware. Thus, this section will focus first on the detection constraints of a space object by an observer and then on the payload electro-optical sensors (EOS) necessary to make that detection with real hardware. This will inform the hardware selection criteria that is laid out in the Materials section. The detection constraints for a constellation of CubeSats for SSA have been laid out in [49] in terms of geometric visualization, line of sight, field of view, and object illumination. This allows for the formulation of the detection of j space objects with i observers as a multivariable nonlinear optimization problem with the system constraints depicted in the images below. The major tenets of the mathematical modeling and system bounding of a CubeSat system for electro-optical detection of space object are laid out in the subsequent pages as were presented in [49].

The line-of-sight vector $\boldsymbol{\rho}_{ij} = \mathbf{r}_j - \mathbf{o}_i$, where \mathbf{r}_j is the j^{th} SO inertial location and \mathbf{o}_i is the i^{th} observer (sensor platform) location. Additionally, $\hat{\mathbf{s}}$ is defined as the sun-vector (pointing away from the sun) and ϕ_{ij} is defined as the solar phase angle of the j^{th} SO as seen by observer i . The i^{th} observer's EOS has a defined boresight $\hat{\mathbf{p}}_i(\boldsymbol{\theta}_{\mathcal{N}}^{\mathcal{O}_i})$, where $\boldsymbol{\theta}_{\mathcal{N}}^{\mathcal{O}_i}$ defines a rotation in SO(3) from the inertial frame \mathcal{N} to the i^{th} EOS boresight frame \mathcal{O}_i .

The j^{th} SO position \mathbf{r}_j and velocity $\dot{\mathbf{r}}_j$ are collectively referred to as the state $\mathbf{x}_j^T = [\mathbf{r}_j^T, \dot{\mathbf{r}}_j^T]$. Similarly, the observing platform state is written as $\mathbf{x}_{o,i}^T = [\mathbf{o}_i^T, \dot{\mathbf{o}}_i^T]$. The states \mathbf{x}_j and $\mathbf{x}_{o,i}$ are restricted over a domain \mathcal{X} such that $\mathbf{x}_j, \mathbf{x}_{o,i} \in \mathcal{X} \subseteq \mathbb{R}^6$. Intuitively, not all possible states $\mathbf{x}_j, \mathbf{x}_{o,i}$ in \mathcal{X} lead to a detection by an EOS on observer i at every instant t , reducing the set of states that may be detected to $\mathcal{D}_i \subseteq \mathcal{X} \subseteq \mathbb{R}^6$. A notional visualization of selected constraints is given in Figure 2.1.

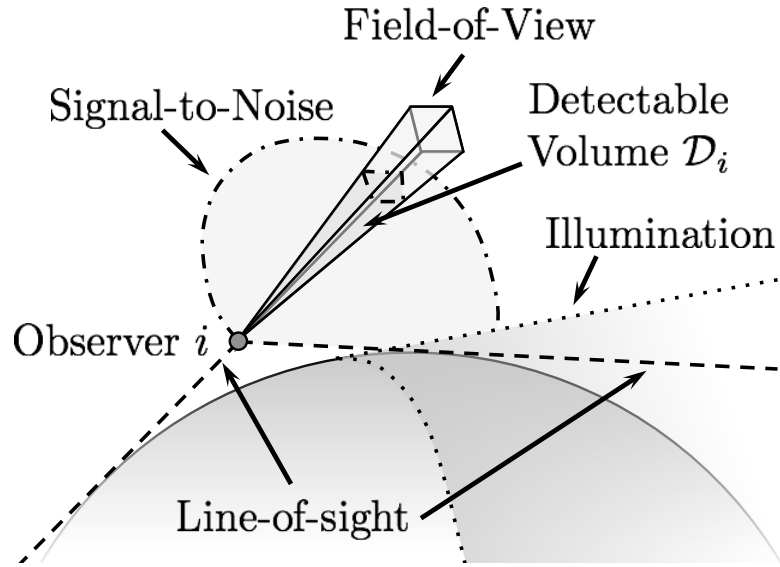


Figure 2.1: Observer i and space object j geometry

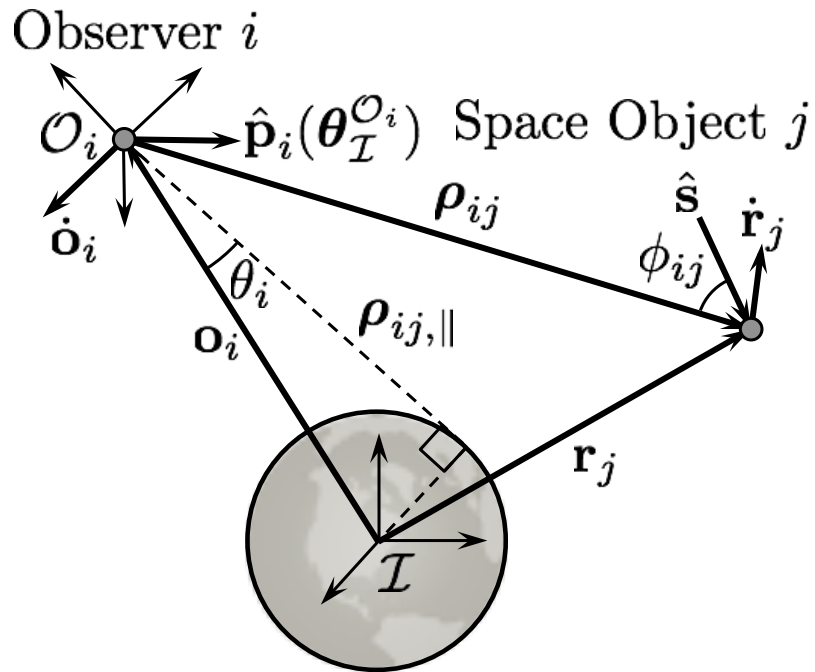


Figure 2.2: Visualization of detectable volume

By bounding the geometric constraints of the system, the design is then freed to work on the optical train and system payload. This leads [49] to build on the work of [7] and fully develop an equation for the probabilistic detection of a space object given electro-optical parameters of a payload sensor.

As demonstrated by Coder & Holzinger [7], the probability of detection for the j^{th} space object (SO) moving relative to the i^{th} sensor frame is given by

$$p_{i,j,d}(t_I; \cdot) \approx \frac{1}{2} \left[1 - \operatorname{erf} \left(\frac{\operatorname{SNR}_{i,\text{alg}} \sqrt{q_{j,\text{SO}} t_I + m_{ij} \left(1 + \frac{1}{z_{ij}}\right) \left[(q_{i,\text{p},\text{bkg}} + q_{i,\text{p},\text{dark}}) + \frac{\sigma_{i,r}^2}{n_i} \right]} - q_{j,\text{SO}} t_I}{\sqrt{2q_{i,\text{SO}} t_I}} \right) \right] \quad (2.1)$$

where $\operatorname{SNR}_{i,\text{alg}}$ is the signal-to-noise ratio required by the detection algorithm, $q_{j,\text{SO}}$ is the EOS count rate generated by the j^{th} space object, $t_{I,i}$ is the i^{th} EOS integration period, m_{ij} is the number of pixels the space object streak covers, z_{ij} is the number of pixels over which the background noise is determined, $q_{i,\text{p},\text{bkg}}$ is the per-pixel EOS count rate due to background sources, $q_{i,\text{p},\text{dark}}$ is the per-pixel count rate due to dark current, $\sigma_{i,r}$ is the EOS read noise, and n_i is the number of image frames per integration period t_I . The EOS count rate $q_{j,\text{SO}}$ is a function of the SO shape, surface materials, inertial location \mathbf{r}_j , and attitude. A full discussion is given by Holzinger, et al. [20].

A parametric design effort is necessary to fully define all of the parameters, but if the fraction of all SOs detected by the constellation in terms of SO parameters and environmental conditions \mathbf{z} for a time interval T can be defined as $\tilde{F}_N(\mathbf{z}, T)$, the optimization problem can then be laid out as such:

Problem 1 (Space Situational Awareness Constellation Optimization). *Determining an SSA constellation of passive EOS sensors (ground-based, space-based, or both) that maximizes the unique detections over a time interval T is equivalent to the following optimization problem:*

$$\begin{aligned} \min_{N, \mathbf{z}} J(N, \mathbf{z}, T) &= -\tilde{F}_N(\mathbf{z}, T) \\ \text{subject to: } \dot{\mathbf{z}} &= \mathbf{f}_z(\mathbf{z}, t), t \in T \\ \mathbf{z} &\in (\mathcal{X} \times \text{SO}(3) \times \mathbb{R}^3 \times \mathcal{P}) \times N \\ N &\in \mathbb{N} \end{aligned}$$

where N is the number of spacecraft, $\mathbf{f}_z : \mathbb{R} \times T \rightarrow \mathbb{R}$ captures any dynamics of the inertial state, orientation states, and parameters for all N spacecraft, $\mathcal{Z} \equiv (\mathcal{X} \times \text{SO}(3) \times \mathbb{R}^3 \times \mathcal{P}) \times N$ defines the set of admissible decision parameters for all N spacecraft, and \mathbb{N} is the set of natural numbers. The decision variable \mathbf{z} is composed of inertial observer states $\mathbf{x}_{o,i}$, orientation states $(\boldsymbol{\theta}_N^{\mathcal{O}_i}(t), \boldsymbol{\omega}_N^{\mathcal{O}_i}(t))$, spacecraft design parameters $\mathbf{d}_i \forall i = 1, \dots, N$.

Having defined the detection problem, the CONOPS of a CubeSat constellation can be used to define further parameters of the optimization problem and make decisions regarding the optical payload.

To design an attitude trajectory through $SO(3)$ for each observer EOS, i , it is helpful to first revisit the principal geometric constraints satisfied as preconditions to each detection. Namely, a SO must be 1) within line-of-sight, 2) within the field of view, and 3) illuminated. Naturally, one may assume that to detect the largest number of SOs, the EOS should be oriented towards regions of illuminated space that do not have the Earth, moon, or sun in the background and are relatively dense with debris. Just such a set of locations are the volumes of space above the north and south poles. Both regions possess the largest spatial density of space objects [50], and also have large fractions of the debris fields from recent on-orbit collisions and explosions. Conversely, very few spacecraft have been launched in to extremely low inclinations (below 20 degrees, for example), so while high inclination satellites pass through this region twice per orbit, there is little incentive to search for space debris in the volume of space near the equator. Lastly, the majority of debris is in LEO, so an attitude trajectory consistent with detecting high inclination LEO objects is preferable.

If the constellation is concerned with detecting LEO space objects, the EOS sensors should be placed in or near LEO to maximize the number of detections (recall that reflected / emitted photon flux collected by EOS i drops off as $1/\rho_{ij}^2$). With these facts in mind, it is determined here that periodic attitude trajectories wherein each EOS i observes volumes at or near the north and south poles provides the largest quantity of unique detections. Therefore, the attitude trajectory is chosen as follows:

1. After passing through its ascending node, EOS i should align its FOV towards the volume of space above the north pole with the highest spatial density of SOs and the smallest possible solar phase angle ϕ_i to a point within the volume (if it satisfies the LoS constraint).
2. Pointing at this volume of space should continue until the LoS constraint is no longer satisfied, or until the descending node is reached
3. After passing through its descending node, EOS i should maneuver to align its FOV towards the volume of space above the south pole with the highest spatial density of SOs and the smallest possible solar phase angle ϕ_i to a point within the volume (if it satisfies the LoS constraint).
4. Pointing at this volume of space should continue until the LoS constraint is no longer satisfied, or until the ascending node is reached, at which time Step 1 should be repeated.

There are many areas of improvement that may be considered, particularly if additional objective functions are defined. For example, an operator may not care only about the number of unique detections, but potentially the frequency of detections or detections for underrepresented populations in existing catalogs or statistical models [50]. If this is the case, then clearly the CONOPS defined here should be revisited.

2.2 Materials

The materials selection for any space mission is concerned first with how the payload will function. After the selection of hardware has been completed for the payload, the results

section will investigate how the supporting flight hardware and systems can be designed to create a functional spacecraft.

2.2.1 Payload Hardware Selection

SSA mission architectures dictate a need to detect as many objects as possible, detect the dimmest objects possible, and obtain detections with as much accuracy as possible, providing criteria by which the system's optical sensor can be sized. While many parameters affect the performance of an optical sensor, aperture diameter D , pixel size p , and focal length l are the most dominant parameters used to quantify the performance of a given optical system [7]. Integration time may be used in conjunction with these optical parameters to determine the cadence of image acquisition for the system to detect objects of a given magnitude. An analysis on these sizing parameters can be used to narrow prospective optics choices, but is not considered an absolute means to obtain a final system design.

By leveraging the three parameters stated above, the instantaneous field of view (IFOV), the field of view of a single pixel, for a given optical system can be defined, where ν refers to f-number, a commonly used parameter for describing optical systems.

$$\nu = l/D \quad (2.2)$$

$$\text{IFOV} = 2\arctan\left(\frac{p}{2\nu D}\right) \quad (2.3)$$

IFOV can be described as the FOV for a single pixel. This parameter is important in determining the overall FOV for an optical sensor, as well as determining the accuracy of a system. The following equation shows how to calculate the vertical and horizontal components of FOV, FOV_v and FOV_h respectively, where n_p is the number of pixels in a given sensor in each direction.

$$\text{FOV}_v = n_{p,v}\text{IFOV} \quad (2.4)$$

$$\text{FOV}_h = n_{p,h}\text{IFOV} \quad (2.5)$$

Optical systems with larger FOVs can view larger areas and thus are capable of detecting a larger volume of objects, N_C , per frame; however, because a sensor with a larger IFOV is capturing photons from a larger area, the precise location of any detected object is less accurately defined. As a result, a tradeoff must be made between detection of more objects, which is achieved with a higher FOV, and accuracy of detections, which is achieved with a lower IFOV, which in turn affect all three of the design parameters, D , l , and p . The impact of this tradeoff can be mitigated by choosing a sensor with a higher number of pixels, but consideration then needs to be given to other aspects of the sensor design such as power draw, physical dimensions, and computational requirements. Additionally, a higher FOV sensor is capable of detecting objects with higher relative angular velocities [42].

To quantify the limiting magnitude, or dimmest signature observable by an optical system, a metric for limiting magnitude needs to be defined. In the below equation, m_v is the

limiting magnitude.

$$m_v = -2.5 \log_{10} \left[\frac{\text{SNR}_{i,\text{alg}} [\sqrt{m_{ij}} \dot{\eta}_{ij} \nu D (q_{i,p,\text{bkg}} + q_{i,p,\text{dark}})]^{\frac{1}{2}}}{\Phi_0 \tau_{\text{atm}} \tau_{\text{opt}} (\frac{\pi D^2}{4}) \text{QE} \sqrt{p}} \right] \quad (2.6)$$

The above equation, developed by Coder and Holzinger [7], incorporates a minimum detectable signal to noise ratio (SNR), which is defined as the ratio of photons emitted by the target object to the photons emitted by all other noise sources. m_{ij} is the number of pixels occupied by photons from SO j as seen by EOS i , $\dot{\eta}_{ij}$ is the apparent angular rate between the sensor motion and the space object, $q_{i,p,\text{bkg}}$ is background radiant intensity per pixel, $q_{i,p,\text{dark}}$ is dark current per pixel, Φ_0 is the spectral excitement of a magnitude 0 object, τ_{atm} is atmospheric transmittance, τ_{opt} is optical transmittance, and QE is the quantum efficiency of a given sensor. Again, a higher limiting magnitude indicates that dimmer objects can be detected, so it is desirable to maximize this value. In terms of design parameters, this implies a longer focal length l , and lower aperture diameter, D .

Given a 6U CubeSat structural architecture, the two largest aperture diameter lenses allowed are 10cm (1U) on the smaller faces and 20cm (2U) on the largest faces as illustrated in Figure 2.3. While both 1U and 2U diameter aperture options are physically possible

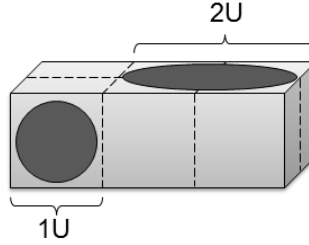


Figure 2.3: 1U and 2U aperture design options for a 6U CubeSat.

on a 6U CubeSat, each case involves additional constraints. Because lenses with 20cm diameters and multiple mirrors are not available off-the-shelf, the focal length of a 2U diameter lens's optical system could be at maximum 10cm, requiring an f-number of less than 0.5. If such optical trains become available in the future, the 2U diameter aperture case could be revisited as an attractive alternative, but is not considered in this analysis. The 1U diameter aperture case allows a focal length of up to 30cm, or an f-number of less than 3. Secondary mirrors are ruled out of the 1U case because with increasing f-number, FOV decreases which results in fewer object detections. Because of the availability of commercial-off-the-shelf (COTS) lens options which satisfy the 1U aperture requirement, this paper focuses on the 1U case. A sample of COTS lens components that fit within the 1U diameter limit, outlined in Table 2.1, are examined to find a suitable component within the design space.

Table 2.1: Sample COTS Lens components

Lens	Focal length (mm)	F-Number, ν	Aperture diameter, D (mm)
ThorLabs MVL50HS ¹	50	0.95	52.6
Kowa LM60JS5MA ²	60	0.8	75.0
Lensagon CM5014GS ³	50	1.4	35.7
Edmund Optics ⁴	75	1.8	41.7
Utopia point	300	3	100

Camera to lens connection mounts are standardized in industry, meaning that if a camera and lens have differing mounts an adapter can be found to make the components compatible. For this reason, lenses and cameras can be examined separately without paying special consideration to the type of mount. Also, as seen in the table above, the Kowa LM60 lens has a significantly larger maximum aperture diameter compared with the other sample lenses. While this provides an advantage in the amount of light the lens can collect, a decision cannot be made until all possible sensor and lens combinations are examined to determine the system’s IFOV, FOV, and limiting magnitude. A sample of COTS components capable of working in a 1U constraint, not considering the camera’s axial direction, are examined as seen in Table 2.2.

Table 2.2: Sample COTS sensor components

Sensor	Pixel size (μm)	Resolution ($n_{p,h} \times n_{p,v}$)	Quantum Efficiency
Photonis Nocturn XL ⁵	9.7	1280×1024	0.60
Pointe Grey Flea3 GE-14S3M-C ⁶	4.65	1384×1032	0.53
Toshiba IK-HR1H ⁷	5	1920×1080	0.60
Gomspace NanoCam C1U ⁸	3.2	2048×1536	0.36
Utopia point	10	10000×10000	1.00

By holistically evaluating the different parameters presented in the equations for optical train performance and the probability of SO detection, the ThorLabs MVL50HS and Photonis Nocturn XL were selected as the payload flight hardware for this flight project.

¹via www.thorlabs.com; accessed 3/30/2017

²via www.kowa.eu; accessed 3/30/2017

³via www.lensation.de; accessed 3/30/2017

⁴via www.edmundoptics.com; accessed 3/30/2017

⁵via www.photonis.com; accessed 3/30/2017

⁶via www.ptgrey.com; accessed 3/30/2017

⁷via www.toshibacameras.com; accessed 3/30/2017

⁸via gomspace.com; accessed 3/30/2017

CHAPTER 3 RESULTS

3.1 Requirements Design

The design of an actual mission can be defined as results of the abstract mission profile design process. The first portion of the spacecraft design to be closed was the requirements definition. These requirements include everything from the high-level mission objectives to the individual system and subsystem requirements for functional operation on-orbit. The requirements definition process was driven by the hardware necessary to accomplish the mission objective of detecting and tracking space debris using an on-orbit sensor. While the formulation of the multi-objective optimization problem presented in the previous section was useful for the payload design, the scope of the problem must be presented more qualitatively to help guide the system design. The mission objectives and requirements that were decided upon are presented in the following tables. From these objectives and requirements, minimum mission success criteria can be developed against which the success or failure of the mission can be measured.

Table 3.1: RECONSO Mission Objectives

MO-1	Detect transient objects within the passive sensor's field of view
MO-2	Compute detected object inertial bearings relative to the RECONSO Spacecraft
MO-3	Track objects as they pass through the field of view during consecutive frames
MO-4	Perform analysis on the ground to generate track information
MO-5	Assess capabilities for on-orbit identification of objects

As a spacecraft designed for the detection of space objects, it should be noted that the mission design requirements are first and foremost developed around the detection of those objects within the field of view. The nature of detecting previously undetected space objects is such there is no specified location within which the observer should search other than broad regions wherein it is expected there may be a higher spatial density of space objects relative to other regions. Given that there is no need for RECONSO to actively search for and track specific objects, the mission objectives can include the word "passive" and eliminate the need for precise and rapid attitude actuation systems on board the spacecraft. However, the simple detection of these objects is not enough because an optical sensor has no way to determine the distance of an uncharacterized object with a single camera. Thus, tracking is defined as an event where an object is detected in a number of consecutive frames to allow for a change in its position over a given amount of time and for rough predictions regarding its propagation forward and backwards in time to be made. The actual number that was used in the design of payload algorithms for these efforts was three consecutive frames. The on-orbit processing of these objects, through the use of various tracking algorithms as well as position and attitude knowledge of the spacecraft enables

the use of a CubeSat form factor by lowering the requirements for data transmission to the ground. If the spacecraft simply took a large amount of pictures and transmitted each high definition picture to the ground for image processing and object tracking, the data throughput and power requirements would be so large as to prohibit the operation of the satellite from something smaller than a several hundred kilogram spacecraft platform.

Table 3.2: RECONSO Mission Design Requirements

MD-1	The duration of the primary mission shall be 6 months.
MD-1.1	Maneuvers, RF communications, deployables, nor any other high risk activities are permitted during start up operations (i.e. not before T+1 week)
MD-2	The RECONSO CubeSat shall deorbit within 25 years from end-of-life
MD-3	The RECONSO CubeSat shall be able to detect transient objects when in an altitude between 300km and 1200 km
MD-4	Maintain exclusion zone around Earth, Moon, and Sun to allow for object detection
MD-5	Reported Inertial bearing uncertainty shall be less than 50 arcseconds (an order of magnitude smaller than MSC-3 to assure success), 3-sigma, including all biases and noises
MD-6	Correlate objects from frame to frame with 95% Confidence

The mission design requirements focus on various engineering decisions that can be made to increase the probability of a successful and feasible mission. These requirements were developed in tandem with the mission success criteria in order to ensure that the spacecraft would be designed in such a way that a concrete goal could be defined that would be carried out with a very high degree of certainty. The primary mission duration was set such that the mission could assuredly be accomplished with good design and hardware could be chosen that would not be prohibitively expensive. With the space object environment in Earth's orbit characterized as precisely as it currently is, a 6 month observation period is ample time to detect a large number of space objects with the naked eye, so a spacecraft that has been effectively designed with that intention in mind should have absolutely no problem accomplishing the task at hand. A large majority of spacecraft hardware has been developed to have very long operational lifetime with high duty cycles, but the 6 month window means that CubeSat and non space-rated hardware can be used without detriment to mission longevity. The exclusion zone is designed to protect the spacecraft optics from unnecessary exposure that is not vital to the mission goal of detecting unknown space objects. The deorbit requirements are designed to fit within regulatory best-practices and also to bound the spacecraft to an orbit where it will not need external hardware to deorbit. This also decreases the amount of hardware necessary to carry out the mission and thus makes the design easier for a CubeSat platform. The confidence in the payload data and accuracy of the payload sensors are bounded to define the order of magnitude of optical performance necessary for the system to carry out the mission. The specified range ensures that the payload data will be both necessary and impactful to the space object catalog and community.

The mission success criteria bounds the performance of the payload such that the size,

Table 3.3: RECONSO Mission Success Criteria

MSC-1	Detection of objects with apparent visual magnitudes better than 7 with passive optical imager
MSC-1.1	Detection of objects with apparent visual magnitudes better than 10 with passive optical imager
MSC-2	Determine and record detected object's visual apparent magnitude
MSC-3	Reported Inertial bearing uncertainty shall be less than 500 arcseconds, 3-sigma, including all biases and noises
MSC-4	Identify the same object in consecutive frames
MSC-5	Determine uncorrelated tracks for objects detected
MSC-6	Downlink 1 object during primary mission lifetime
MSC-6.1	Downlink 1 track (correlation on the same object with 95% confidence in 3 consecutive frames) during primary mission lifetime
MSC-7	Associate detected objects with a catalog of known objects through on-orbit analysis.

quality, and cost of the optics can all be easily defined and can fit within the expected performance of a 6U CubeSat system. Additionally, the use of RECONSO as a mission to prove the concept of on-orbit space debris from a COTS CubeSat system allows for the creation of success criteria that determine the mission to be a success after just one object has been successfully detected and tracked to within the degree of certainty and confidence that would be of use to the space-debris tracking community. The visual magnitude requirement bounds the objects that can be detected such that the detection of one such object would prove that the system would contribute in a meaningful way to the space object catalog by detecting the class of object that is currently missing from the catalog. The final success requirements to associate detected objects with a catalog of known objects allows the performance of the system to be verified against existing data. This not only allows for a measure of verification for the system, but also demonstrates that the system can be used by third parties to capture meaningful SSA data for purposes of maneuver detection or tasked tracking.

The requirements presented here were designed to be both quantitative and easily measurable through various verification techniques, such as inspection, design, or analysis. They were then flowed down to create the requirements for individual systems and subsystems, resulting in over 200 requirements in total. Due to the large number of requirements, these requirements are not presented here.

CHAPTER 4 DISCUSSION

Having defined the parameters of the system, the process of hardware selection was then begun. A number of different avenues were pursued to acquire hardware - funding from the Air Force Research Lab (AFRL) was used, donations were sought from various companies, and arrangements were made with existing flight projects at Georgia Tech that had extra hardware. There were two different hardware trades that had to be closed between the attitude determination and control subsystem (ADCS), the command and data handling subsystem (CDH), the telecommunications subsystem (COM), and the electrical power subsystem (EPS). Each of these trades was bounded by the technical budgets and requirements flowed down from the mission objectives, design requirements, and minimum success criteria.

4.1 ADCS Trade

Having been designed based on various COTS baseline components, the preliminary RE-CONSO ADCS hardware design was chosen as is listed below at the start of the trade.

Table 4.1: Initial status of ADCS hardware

Magnetometer	In-house construction
Sun Sensors	Elmos E910.86 sun angle sensors
IMU	Analog Devices ADIS16360
Star Tracker	Payload camera and in-house software
GPS Receiver	Surrey Space SGR-05U with antenna
GPS Antenna	N/A
ADCS Microcontroller	ISIS OBC

The components that will be reexamined in this trade are presented along with their reason for reexamination in the table below.

It should also be noted that the IMU provided the same functionality as the 6 degree-of-freedom accelerometer that was already on-board the Tyvak Intrepid flight computer, which had already been chosen prior to the opening of this trade. As monetary budgets and development timelines were taken into account, various aspects of the system hardware design had to be reexamined to determine whether or not they were necessary for system functionality or would simply end up driving up programmatic costs and timelines without a significant impact on mission functionality. Initial hardware choices were based off of industry-standard COTS components and little to no consideration was given to ease of use, system integration, and industry-standard costs. Traditional space-rated hardware is often excessively expensive in a manner that is not commensurate with the value added by the component.

Table 4.2: Reasoning for opening trade on each component

Component	Reasoning for Reexamining
Sun Sensors	Elmos E910.86 sun sensors have gone out of production and Elmos no longer makes a similar product
IMU	Analog Devices has discontinued the ADIS16360 model and replaced it with a newer version
GPS Receiver	At a price point of \$22,000, the SGR-05U is not feasibly within the project's budget. It was chosen without cost as a driving constraint.
GPS Antenna	The majority of GPS receivers do not come with an antenna included
ADCS Microcontroller	The ISIS OBC offers far more computing power than is necessary for this application and can thus be replaced by cheaper hardware

4.1.1 Objectives of trade

This section will outline the current status of each element of the trade study along with the applicable decision criteria.

Sun Sensors

The sun sensors will be used along with the on-board magnetometer to perform coarse attitude determination in the data processing or safety modes of the satellite. While in the data processing or safety mode, the camera will be turned off and thus not available for star-tracking, the most accurate and primary form of attitude determination that the spacecraft will be utilizing. 6 different sensors will be placed on the satellite structure with one sun sensor on each face. The angle of incident solar light measured by each sensor will be fed into an on-board algorithm running on the ADCS Microcontroller. It should be noted that the accuracy of the sun sensors is not the most crucial systems-level constraint for this sensor. This is because there is no mode of operation in which the sun sensors will be running without the magnetometer running as well. These two sensors together are only designed to accomplish coarse attitude knowledge such that the spacecraft can ensure that the boresight of the camera is not pointed at any of the zones of exclusion within 10 degrees RMS. In short, there is no fine pointing knowledge that the ADCS system will need to acquire while the star tracker (the most reliable form of attitude knowledge) is not available.

The top three systems level constraints that will be taken into account for the sun sensors are as follows (in order of importance).

1. Compatibility with existing structure - The chosen sun sensors will need to be mounted on the exterior of the satellite to be of any use. Space on the outside of the spacecraft structure is at a premium given the fact that the external surface will also be covered with solar cells and every solar cell is necessary to allow the current power budget to close on each orbit. Antennas are also more important than sun sensors and absolutely must be on the exterior of the spacecraft.
2. Cost - The chosen component must fit within the remaining budget of the project. Sun

sensors can vary from cheap photodiodes to flight-tested, multiple thousand dollar components.

3. Flight heritage/Reliability - The sensors flown on the spacecraft must be a proven and reliable system to ensure accuracy throughout the 6 month primary mission duration.

Inertial Measurement Unit

The Inertial Measurement Unit (IMU) will be responsible for measuring linear and angular accelerations of the spacecraft. This data will be used to determine changes in the linear and angular position and attitude of the spacecraft in the ECI frame and the actuation of magnetorquers necessary to correct the attitude of the spacecraft at any given time. This system was chosen to add a level of redundancy and higher accuracy to the IMU already on board the Tyvak Intrepid primary flight computer. The necessity of higher-order accuracy that the existing sensor will be weighed against the subsequent increase in system complexity, power, and cost that this component provides. The trade for the IMU take the following parameters into account (in order of importance):

1. Accuracy/Reliability - Must be of sufficient use to the spacecraft design to justify an increase in system complexity and cost
2. Structural compatibility - Must be a small enough sensor to fit in the existing structure with the existing components

GPS Receiver

The GPS Receiver will be used to determine the ECEF position and velocity of the spacecraft immediately after deployment and throughout the mission. The GPS Receiver and IMU will be used together to determine these two measurements as accurately as possible. An accurate position and velocity of the spacecraft at time of space object detection is crucial to the creation of a valuable data product that has low track uncertainty and high correlation confidence. The decision parameters for the GPS Receiver are as follows (in order of importance):

1. Accuracy - An accurate position and velocity measurement of the spacecraft is crucial to communicating with the spacecraft, creating a valuable data product, and avoiding zones of exclusion.
2. Cost - GPS Receivers vary widely in cost, and the option chosen must fit within the existing project budget.
3. Structural compatibility - Many popular GPS receivers are made for Microsat-class missions and are thus structurally incompatible with the 6U form-factor of RE-CONSO.

GPS Antenna

The GPS Antenna must be chosen such that it is compatible with the chosen GPS receiver. It will be mounted on the zenith-pointing exterior of the spacecraft structure so that it has the best possible connection to the GPS constellation. Cost is not considered a driving consideration for this component as GPS receivers are often paired with GPS antennas on a similar order of magnitude cost. The decision parameters for the GPS Antenna are as follows (in order of importance):

1. GPS Receiver compatibility - The antenna absolutely must work properly with the receiver.
2. Structural compatibility - The antenna must fit properly on the exterior of the satellite where space is at a premium for power generation and sun sensing.

ADCS Microcontroller

The ADCS Microcontroller will interface with all of the ADCS hardware and run the A/D filter and estimator to determine estimates for the position, velocity, and attitude of the spacecraft. This state estimation will be fed to the Tyvak primary flight computer for use in determining mode, health, and CONOPS decisions of the flight software. The ADCS microcontroller is similar to the IMU in that it could be replaced by the Tyvak Intrepid - there are ample GPIO ports on the Tyvak Intrepid to allow for the connection of all ADCS hardware and the Tyvak Intrepid provides enough processing power to carry out ADCS operations along with the rest of the flight software. Given that all of these functionalities could also be implemented on the Tyvak Intrepid primary flight computer, the ADCS microcontroller must also offer sufficient benefits in terms of ease of software development, hardware I/O, and system integration in order to be justified for use with the existing system. The decision parameters for the ADCS Microcontroller are as follows (in order of importance):

1. Compatibility with existing hardware - The ADCS Microcontroller must have the right type and number of data connections to interface with all ADCS components and the primary flight computer.
2. Ease of development - The Microcontroller should ideally be an open-source development environment such that custom libraries can be easily installed and there is a short learning curve for students developing on the board.
3. Cost - The Microcontroller should fit within the existing project budget.

4.1.2 Trade evaluation

This section will evaluate each of the decisions presented in the previous section according to the various performance criteria that were presented for each trade. Accommodation with the existing system will be taken into account for each decision and an extra emphasis

on the compatibility with various subsystems will be given when necessary. Project management (MGT) will also be taken into account to evaluate price and schedule effects on the project.

Evaluation of Sun Sensors

The RECONSO mission has already proven a brass-board prototype for the sun sensor hardware. This was done with photodiodes placed on the sides of a cardboard box, GPIO pins interfacing with an Arduino, and the control logic running on Texas Instruments Tiva C Series Launchpad microcontroller running Linux. The accuracy of these sensors has not yet been quantified, but it does prove that the software integration of whatever sensors are chosen will not be a large consideration for whatever option is chosen, as the software will not likely change much between the brass-board and gold-board components.

The baselined component, Elmos E910.86 sun angle sensors must be replaced as they are no longer in production and Elmos does not manufacture a similar product.

The following options will be evaluated:

1. NSS CubeSat Sun Sensor ¹
2. Maryland Aerospace Inc. Sun Sensor
3. In-house Photodiodes



Figure 4.1: NSS CubeSat Sun Sensors



Figure 4.2: MAI Sun Sensors

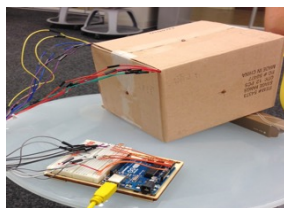


Figure 4.3: In-house brass-board prototype of photodiode sun sensors

Impacts on STR

The dimensions of each component along with their mounting specifications are listed in the table below.

Each sensor is evaluated according to various decision parameters in the table below.

¹cubesatshop.com; accessed 3/30/2017

Table 4.3: Dimensions of different sun sensor options

Component	Dimensions	Mounting	Field of View
NSS CubeSat Sun Sensor	33mm x 11mm x 6mm	3 x 4-40 screws	114°
MAI Sun Sensor	2" x .875" x .275"	4 x 4-40 screws	57°
In-house Photodiodes	7mm x 7mm x 3mm	soldered to solar panel	90°est.

Table 4.4: Sun sensor technical specifications

	NSS CubeSat Sun Sensor	MAI Sun Sensor	In-house photodiodes
Accuracy	$\pm .5^\circ$	$\pm 3^\circ$	$\pm 10^\circ$ est.
Cost	\$3,300 per sensor	\$990 per sensor	\$5 per sensor
Reliability	High	High	Low

Impacts on STR/EPS

Given that each of these sensors requires mounting on the outside faces of the satellite to be of any use, the main factor that will need to be taken into account for integration with the existing system is whether or not they will require a changing of the solar panels. The solar panels have already been optimized in the solar panel trade study such that the maximum number of cells that fits on each panel generates enough power for the power budget to close on each orbit. The reduction of power generation capability that would be caused by needing to rework the panels and put fewer cells on them would be a serious detriment to the spacecraft's operational capacity.

It should also be noted that some sensors are active while others are passive. The NSS CubeSat Sun Sensors and one configuration of the MAI Sun Sensors require power to operate and output a change in voltage in response to the incident sun angle on the sensor. The secondary configuration of the MAI sensors and photodiodes simply output a current in response to the magnitude of the incident sunlight. Passive sensors are preferable from an EPS perspective as they would create less of an overall impact on the EPS power budget.

Impacts on MGT

The time to acquire each of these components varies widely. Both the NSS and MAI require 1-3 months to acquire. The in-house photodiodes would take a number of days to acquire, and then approximately a month or two to test and integrate with the existing system. From a management perspective, it is preferable to use photodiodes to fabricate sun sensors in-house.

Conclusion

While the NSS and MAI sun sensors offer more flight heritage and higher reliability than in-house photodiodes, the fact that they are significantly more expensive and come on timescales that are likely much slower than in-house options outweighs these benefits. The RECONSO mission has opted to go with an in-house implementation of COTS photodi-

odes for sun sensing attitude knowledge. By mounting a simple position-sensitive light sensor on the solar panels of the satellite, the coarse attitude of the spacecraft can be determined at any given time. These measurements can be verified by comparing them to the current differential produced by each panel on the spacecraft. Along with the use of the magnetometer for coarse attitude determination in all modes of spacecraft operation, the coarse attitude requirements can be met.

4.1.3 Evaluation of Inertial Measurement Unit

The inertial measurement that was originally selected for the satellite was the Analog Devices ADIS16360. It should be noted that this component was not completely discontinued by the manufacturer; it was simply phased out so that a newer, more accurate and capable sensor could be marketed instead. As such, the newer version is the only other option that will be evaluated for this trade as it is known to already fit within the existing system parameter. The two options will be compared to each other and to the Tyvak Intrepid on-board unit so that it can be determined whether or not the new option is desirable.

1. Analog Devices ADIS16360² (original choice)
2. Analog Devices ADIS16365³ (updated model)



Figure 4.4: Analog Devices ADIS16365

The table below lists the technical specifications required by the component (as per the requirements flowdown) and those available from the ADIS16365. It should be noted that the the flight computer has already been accommodated electrically, structurally, and thermally within the spacecraft system. As such, the only parameters necessary for evaluation of the trade are the angular and linear acceleration ranges. The accelerometer on-board the Intrepid is the BST-BMA250 digital triaxial acceleration sensor⁴ and the gyroscope on-board the Intrepid is the L3G4200D MEMS ultra-stable three-axis digital output gyroscope⁵.

²analog.com; accessed 3/30/2017

³analog.com; accessed 3/30/2017

⁴media.digikey.com

⁵st.com

Table 4.5: IMU technical specifications

	ADIS16365	Tyvak Intrepid on-board unit
Angular rate range	$\pm 300^\circ/\text{sec}$	$\pm 500^\circ/\text{sec}$
Linear acceleration range	$\pm 18 \text{ g}$	$\pm 16 \text{ g}$
Operating temperature	-40°C to 105°C	-40°C to 85°C
Operating voltage	4.75 V to 5.25 V	5V

It can be seen here that the Analog Devices option does not have a very appreciable impact on the inertial measurement capabilities of the system relative to the Tyvak Intrepid on-board sensors.

Impacts on STR

Both Analog Devices components have the same form factor and have mounting holes in the same location, so the change in component is not an issue in terms of volumetric constraints within the spacecraft.

Impacts on CDH/FSW

Both Analog Devices components communicate on SPI, so the use of either component will not affect the system in a large way. The data can easily be passed to the ADCS Microcontroller as long as it is capable of SPI communication. The on-board sensors will have to pass data to the ADCS microcontroller, which will then pass a computed state back to the Tyvak Intrepid, but this software design is not appreciably different than that of any other hardware component on the spacecraft.

Impacts on MGT

The ADIS16365 is available for single unit purchases from a variety of distributors, as well as from Analog Devices itself. At the time of writing, the component is available to ship immediately at a cost of \$560, only slightly more than the cost of the original component and well within the project budget. The on-board sensors come at no additional cost than the flight computer which had already been purchased at the time of this writing.

Conclusion

Given that the two components are so similar and that the technical specifications do not appear to be any different between the original component and the new component, the RECONSO mission has opted to use the simpler and easier design of the Tyvak Intrepid on-board sensors.

4.1.4 Evaluation of GPS Receiver

The GPS Receiver must interface with the GPS constellation to accurately determine a state vector for the satellite in the ECEF frame. This will aid in tracking and communicating with the satellite as well as with creating a valuable data product. Of course, the GPS receiver must also interface with the ADCS Microcontroller, GPS Antenna, and the existing structure of the spacecraft.

The following options will be considered:

1. Skyfox Labs piNAV-L1 GPS⁶
2. Novatel OEM615⁷
3. Pumpkin GPSRM 1 GPS Receiver⁸
4. SSBV Space-based GPS Receiver⁹



Figure 4.5: Skyfox Labs piNAV-L1 GPS



Figure 4.6: Novatel OEM615 GPS



Figure 4.7: Pumpkin GPSRM 1 GPS Receiver



Figure 4.8: SSBV Space-based GPS Receiver

The specifications for each product are listed below:

The data presented in the above table is enough to disqualify the SSBV Space-based GPS Receiver based on the fact that it is still under development. There is currently no pricing information available for the product because it is not currently in commercial production. While that may be acceptable for a component that is less necessary for the mission success

⁶skyfoxlabs.com; accessed 3/30/2017

⁷novatel.com; accessed 3/30/2017

⁸cubesatkit.com; accessed 3/30/2017

⁹ssbv.com; accessed 3/30/2017

Table 4.6: GPS Receiver technical specifications

	piNAV-L1	Novatel	Pumpkin	SSBV
Operating frequency	L1	L1, L2, L2C	L1	L1
Time to first fix	300 sec	50 sec	50 sec	Not Available
Position accuracy	10 m	1.5 m	1.5 m	approx. 10 m
Velocity accuracy	10 cm/s	3 cm/s	3 cm/s	approx. 25 cm/s
Data interface	UART	I2C	I2C	I2C
Physical dimensions	75x35x12.5 mm	46x71x11 mm	96x90x15 mm	50x20x5 mm
Operating voltage	3.3V	3.3V	3.3V or 5V	5V
Power consumption	0.12 W	1 W	1.3 W	Not Available
Operating temperatures	-40°C to +85°C	-40°C to +85°C	-40°C to +85°C	-10°C to +50°C
Cost	\$7,500	\$750	\$7,980	Not Available

and can have a longer timeline to acquisition, it would not be wise to base such a critical mission operation as payload data accuracy on a component that has no flight heritage.

The Skyfox, Novatel, and Pumpkin options are thus both very similar, the primary difference between the two being their power draw. However, the current EPS power budget baselines a 2.5 watt power draw for the GPS based on the Surrey Space option. As such, while the power draw of the Skyfox option is attractive, it is only marginally so. Each of these three options has a similar amount of flight heritage as well [1].

Impacts on STR

As far as structural integration goes, there is ample room for all three remaining components within the existing structure of the spacecraft. The Novatel OEM615 receiver is the best option in this category as it has the smallest form factor and would be the easiest to mount while accommodating harnessing and antenna constraints. However, given the fact that RECONSO has elected to use the SUPERNOVA III 6U structure for the satellite, the GPSRM 1 component will be guaranteed to fit with the existing structure, even though it may have a larger footprint than either of the other models.

Impacts on MGT

While not a technical resource per se, the author believes that it is worth noting that Pumpkin Inc. has been incredibly responsive and helpful in communicating with the RECONSO mission in the past. As a California-based company with a number of Georgia Tech grads as full-time employees, Pumpkin has provided excellent technical support to the project in the past, often returning emails with timely phone calls and making peripheral hardware and software recommendations based on their extensive experience. Skyfox Labs, while making a quality component at a low-cost, is based in the Czech Republic and likely will not be able to provide as helpful of technical support simply due to time zone differences. Additionally, because Skyfox is an international company, there is going to be additional export control paperwork surrounding the purchase of the piNAV-L1 unit.

Given that RECONSO has struggled in the past with communication from suppliers,

the fact that Pumpkin has been so responsive in the past is seen as a positive characteristic of the GPSRM 1 Receiver.

However, it should also be noted that the Novatel OEM615 comes with the lowest price point. While this is not an engineering criteria, it is a benefit to the project as a whole. The Surrey space unit that is being replaced as an initial option in this trade was substantially more expensive than any of these options, so while the savings are attractive, they are not overwhelmingly so. This leaves the OEM615 as a good fallback option should another, more expensive, option not work out as the cost will fit within the project budget regardless.

Conclusion

In conclusion, the decision comes down to a ranking of the piNAV-L1, OEM615, and GPSRM 1 in terms of the original decision criteria. The components will be ranked 1-3 in each of the decision parameters in the table below in an effort to determine the winner.

Table 4.7: GPS Receiver decision

Parameter	piNAV-L1	OEM615	GPSRM 1
Accuracy	3	1	1
Cost	2	1	3
Structural Compatibility	2	3	1

Given this ranking, the RECONSO mission has opted to go with the Pumpkin GPSRM 1, with the OEM615 in mind as a fallback option should the GPSRM 1 not work as initially planned.

4.1.5 Evaluation of GPS Antenna

Having selected the GPS Receiver, the choice of GPS Antenna is highly biased towards the option that is most compatible with the receiver that was chosen. However, in the interest of thoroughness, three options will be compared.

1. AntCom 1.5G15A-18NM-1-S¹⁰
2. Skyfox PocketQube GPS Patch Antenna¹¹
3. Skyfox Space-Friendly CubeSat GPS Antenna¹²

The AntCom 1.5G15A-18NM-1-S is recommended by Pumpkin for use with their GPSRM 1 Receiver. The PocketQube GPS Patch Antenna is designed and manufactured by Skyfox for use with the piNAV-L1 Receiver; likewise for the Space-Friendly CubeSat GPS Antenna and the piNAV-L1 Receiver.

¹⁰antcom.com; accessed 3/30/2017

¹¹skyfoxlabs.com; accessed 3/30/2017

¹²skyfoxlabs.com; accessed 3/30/2017



Figure 4.9: AntCom 1.5G15A-18NM-1-S

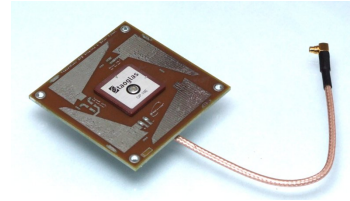


Figure 4.10: Skyfox PocketQube GPS Patch Antenna

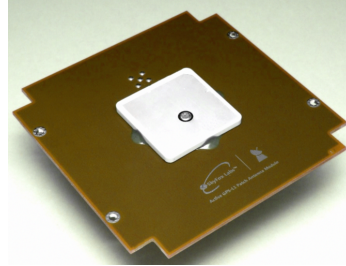


Figure 4.11: Skyfox Space-Friendly CubeSat GPS Antenna

Compatibility with STR

The structures subsystem has left a 1U face of the structure next to the 1U face out of which the boresight of the payload lens will be facing. This component layout is illustrated in the following figure. It can be seen that regardless of the option chosen, the 1U face will be able to act as a grounding plane for the GPS antenna and that there will be plenty of room to mount whichever antenna is chosen. Also labelled are the UHF antenna and the GlobalStar Patch antenna that are mounted on the opposite 2U face and will be used for primary mission telecommunications.

Thus, it can be seen that whichever option is chosen, there will be ample room to mount the GPS antenna. It will also be close enough to the GPS Receiver to ensure that there will not be large losses from the antenna to the receiver due to the length of the cable between the two components.

Compatibility with EPS

All of the above-listed options are active antennas, meaning that they will require some power consumption to operate effectively. The PocketQube Patch Antenna makes the best attempt at remedying this, however, by mounting extra solar cells in the space around the antenna at no extra cost. Although that face of the spacecraft will never be pointed directly at the sun due to the dangers of overexposing the payload camera, there will be a nonzero power generation of those cells due to albedo and other effects. While this is not enough to be easily quantifiable, it is certainly not a negative affect. The low power use by all of the available GPS receivers will also more than make up for any room necessary in the power budget.

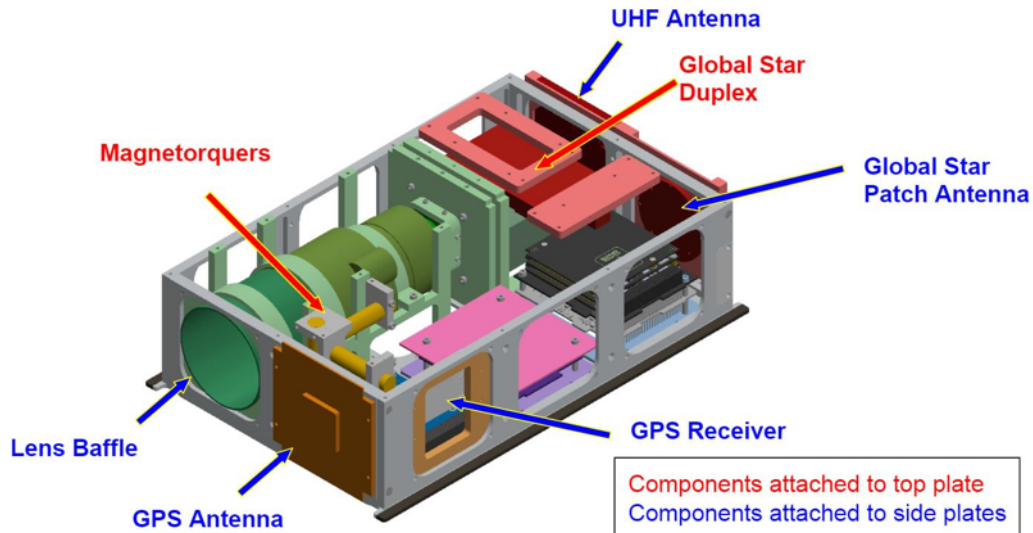


Figure 4.12: Spacecraft structure and packaging of RECONSO

Impacts on MGT

The final decision parameter relevant to this section of the trade is the cost of each antenna. It is here that the Skyfox options have the most advantage, given that they would both come free with the purchase of their associated GPS Receiver. The AntCom antenna would cost approximately \$350, although AntCom sales requires a minimum purchase of \$1,000, so other equipment that is perhaps not as necessary to the project would have to be purchased with the antenna as well.

Conclusion

Although the AntCom option costs more and does not have any built-in solar cells, the fact that it is most compatible with the GPS Receiver that has been chosen is the most important decision criteria. As such, the RECONSO mission has opted to go with the AntCom 1.5G15A-18NM-1-S GPS Antenna.

4.1.6 Evaluation of ADCS Microcontroller

Now that every other piece of ADCS hardware has been decided upon, the ADCS Microcontroller must be chosen to interface with each of the different components. As such, it may now be determined that in addition to the original decision parameters, the ADCS Microcontroller must be able to communicate over:

1. SPI (IMU)
2. UART (GPS Receiver)

As such, the following options may be considered for the trade:

1. BeagleBone Black¹³
2. BeagleBone Black with Pumpkin Motherboard Module (BBB/MBM)¹⁴
3. Innovative Solutions in Space On-board Computer (ISIS OBC)¹⁵

Each of these options is capable of communication over I2C (necessary to communicate with the primary flight computer, the Tyvak Intrepid), SPI, as well as UART. As such, the first design parameter is satisfied equally by all three of these components and is thus disregarded as a merit of relative goodness henceforth. All three options have flight heritage as well, so that will also be disregarded as a merit of relative goodness [1].

Technical Specifications

The following table outlines the technical specifications of each of the available options so that they may be compared with regards to the other decision parameters.

Table 4.8: ADCS Microcontroller technical specifications

Specification	BeagleBone Black	BBB/MBM	ISIS OBC
GPIO Pins	92	92	27
Processor	1GHz ARM Cortex-A8	1GHz ARM Cortex-A8	400MHz ARM 9
Operating System	Debian or Ubuntu Linux	Debian Linux	FreeRTOS
Cost	\$50	\$1,300	\$4,700

Given that all three components satisfy the design parameter of compatibility with existing hardware, the remaining two design criteria are ease of programming and cost. It is here where the BeagleBone Black platforms have the most advantage. As an open-source platform that is very commonly used among students, the Linux operating system offers a huge advantage in terms of schedule and technical risks. All of the libraries that are now to be needed for the ADCS flight software have been programmed in Linux, so the RE-CONSO mission is certain of software compatibility between the BeagleBone Black and the A/D filter. The same cannot be said about FreeRTOS, which students have little to no experience with and would involve a rather steep learning curve before hardware integration could begin.

When considering cost, the BeagleBone Black has the clear advantage again. As was previously mentioned, the ISIS OBC is designed as a full-fledged flight computer, which would appear to be far more than the ADCS Microcontroller will need to be capable of. The Pumpkin BBB/MBM option allows for easier interfacing between the BBB and various other pieces of flight hardware, but given that the BBB is only required to interface with the ADCS components, it is not clear that such functionality will be required immediately or later down the road.

¹³beagleboard.org; accessed 3/30/2017

¹⁴cubesatkit.com; accessed 3/30/2017

¹⁵isispace.nl; accessed 3/30/2017

Conclusion

As it performs better with regards to all of the design criteria, it is clear that the BeagleBone Black standalone option is the best-suited for choice on RECONSO. Additionally, it is known that the PROX-1 satellite mission at Georgia Tech is planning on using several BeagleBone Black computers for all of their on-board computing, so technical support for interfacing such components will be nearby and readily available. The BeagleBone Black is thus the best offering, and the RECONSO mission has opted to go with this component for the ADCS Microcontroller.

4.1.7 Trade Conclusion and Summary

As per the review presented above, the RECONSO mission will be making the following purchases of flight hardware on the attached timelines:

Table 4.9: Final trade decisions

Component	Choice	Cost	Time to acquisition
Sun Sensors	In-house photodiodes	\$50	1 week
IMU	Tyvak Intrepid on-board unit	\$0	None
GPS Receiver	Pumpkin GPSRM 1 GPS Receiver	\$7,980	6-8 weeks
GPS Antenna	AntCom 1.5G15A-18NM-1-S GPS	\$350	6-8 weeks
ADCS Microcontroller	BeagleBone Black	\$150	1 week

4.2 CDH Trade

The Telecommunications (COM) system of a CubeSat is the largest area of mission risk for the vast majority of missions, RECONSO included. The flight hardware that has been planned for use on the RECONSO satellite before the opening of this trade is listed below. The hardware was chosen largely based on the ground station capabilities that were available at Georgia Tech at the time of the initial hardware selection and the compatibility with the existing flight computer.

Table 4.10: Status of COM subsystem before trade

Uplink	Tyvak UHF Daughterboard Tyvak Quad Monopole antenna
Downlink	Astrodev S-Band Transmitter Astrodev Amplifier Astrodev Patch Antenna

Just as important to the functioning of the COM system is the ground station that is used in conjunction with the COM system. The existing plan for the ground station has been to share ground station facilities with the PROX-1 satellite mission, another small satellite mission under development at Georgia Tech at the same time as RECONSO. The hardware that will be used for this purpose is listed below:

Table 4.11: Status of ground station before trade

UHF Uplink	13 foot Yagi antenna Kenwood TS-2000X transceiver
S-Band Downlink	3m diameter mesh dish antenna Kenwood TS-2000X transceiver
Tracking software	NOVA antenna steering HAM radio deluxe satellite tracking

4.2.1 Objectives of trade

This section will outline the current status of each element of the trade study along with their applicable decision criteria.

UHF Antenna

The only aspect of the UHF system that this trade study will examine is the selection of a proper UHF antenna, as the existing option is incompatible with the RECONSO 6U form factor. As of yet, no antenna has been selected for flight use on board the RECONSO spacecraft. The previously considered Tyvak quad-monopole unit will be insufficient as it is designed for a 3U bus and thus the 6U form factor of RECONSO lacks a proper location for its mounting. Given that other COM flight components are currently being finalized and purchased, it was deemed that this is an appropriate time to finalize the selection of this component as well.

The top three systems level constraints that will be taken into account for the UHF antenna are as follows (in order of importance):

1. Structural compatibility - Any antenna selected will need to be structurally compatible with the existing satellite
2. Electrical compatibility - The option chosen must provide sufficiently high gain, sufficiently high RF power, and operate at a voltage that is compatible with the rest of the satellite
3. Flight heritage/Reliability - Must be a proven and reliable system to ensure correct antenna deployment

Downlink System

The S-Band system originally planned to use the Astrodev S-Band transmitter, amplifier, and patch antenna. However, delays in communication, purchasing, and acquisition with Astrodev Inc. have necessitate a change in provider. Astrodev was contacted about a quote in October 2014. The quote was received in January 2015, and the company has stopped responding to communication since that date. Various other S-Band systems will be examined given that the RECONSO mission operations team will have access to an S-Band ground station (see §2.3).

Near Space Launch has also approached RECONSO and the rest of the UNP-8 flight programs with the option of using the GlobalStar satellite communication network. RECONSO can choose to use either a simplex or duplex unit. Both units have been flight tested, operate with a bent-pipe ground system architecture, and will offer subsidized data rates due to the nature of our educational program.

The trade for the entire downlink system will therefore take the following parameters into account (in order of importance):

1. Flight heritage/Reliability - Must be a proven and reliable system to ensure mission success
2. Data rates - Necessary for achieving minimum mission success of downlinking validation images
3. CONOPS compatibility - Any COM system selected will need to be compatible with the STR, TCS, and EPS systems of the satellite as well as the concept of operations.

These parameters are slightly different from the UHF antenna goodness metrics due to the fact that the UHF antenna will already be operating on the Tyvak UHF daughterboard which has been flight tested numerous times.

Ground Station

The Georgia Tech ground station has gone through a number of changes that will influence the selection of COM components for RECONSO. The following changes are currently being made to the ground station that, although they are based more in logistics than engineering decision criteria, represent nontrivial challenges to the project:

Table 4.12: Aspects of ground station opened for trade along with reasoning

UHF Antenna	13 foot single Yagi antenna is in the process of being replaced with 18 foot phased dual Yagi antenna
S-Band System	Being moved from on-campus location on Montgomery Knight building to an off-campus GTRI facility in Marietta, GA
Cabling	Currently very lossy, will need to be replaced with weather-proof option
Computer	COTS mission operations software installed by Georgia Tech IT

The decision parameters for the ground station are as follows (in order of importance):

1. Effectiveness - An effective ground station that will allow communication with the spacecraft in a reliable and frequent manner is essential to mission success
2. Ease of access - Necessary for consistent and fast iteration on integration and testing

There are a number of actions that the RECONSO mission could take to remedy the current status of ground station. The first option would be to create a secondary UHF/S-Band ground station on the roof of the Howey Physics building next to the Georgia Tech observatory, a location that is already in heavy use by our principal investigator, Dr. Holzinger. Another option would be to replace the S-Band system at the Georgia Tech Montgomery Knight building to provide a replacement for the S-Band capabilities that are being moved to Marietta. A third option would be to only use the UHF system that is currently being upgraded and removing all S-Band capabilities from the satellite, either using solely UHF or replacing S-Band with a GlobalStar system.

4.2.2 Trade evaluation

This section will evaluate each of the decisions presented in the previous section according to the various performance criteria that were presented for each trade. Accommodation with the existing system will be taken into account for each decision, with a special emphasis on the Structural (STR), Electrical (EPS), and Command & Data Handling (CDH) subsystems. Project management (MGT) will also be taken into account to evaluate price,

Evaluation of UHF Antenna

The RECONSO CubeSat is making every effort possible to stick to commercially available off-the-shelf (COTS) components that can be purchased from reliable providers. As a result, most of the options that will be examined here are components that can be bought, not custom hardware that would be created in-house.

The following options will be evaluated:

1. ISIS Deployable UHF Antenna for CubeSats ¹⁶
2. GOMspace AT430 UHF Turnstile Antenna ¹⁷
3. In-house tape measure UHF monopole antenna

Impacts on STR

There are two constraints as to the faces of the satellite upon which the UHF antenna can be mounted. Firstly, the placement of the antenna will have to preserve area for as many solar cells as possible so that power generation is not affected by the use of the antenna. Secondly, the antenna cannot be placed on the same 2U face of the satellite from which the optical train points. For whichever option is chosen, the highest gain will result from pointing the long axis of the antenna towards the earth to communicate with the ground station. Given that a zone of exclusion must be kept around the earth to prevent overexposure of the optics, the UHF antenna must not be placed on the same 2U face as the optics. The 3U and 6U faces afford the greatest solar panel surface area and are most

¹⁶cubesatshop.com; accessed 3/30/2017

¹⁷gomspace.com; accessed 3/30/2017

likely to be pointed towards the sun for maximum power generation. This leaves the 2U face opposite the optical train as the only possible candidate for antenna placement.

The ISIS Deployable UHF Antenna is shown below in Figure 4.13. The configuration shown is the quad turnstile version, but the form factor holds for all available configurations: Quad monopole, single dipole, dual dipole, turnstile, and monopole + dipole. All of these options deploy using a doubly redundant 50Ω burn-wire that automatically activates upon successful satellite deployment. Given the 6U form factor of the RECONSO satellite, it is evident that the quad turnstile configuration will not be a good fit for the satellite. However, the single dipole configuration or the single monopole configuration, with the component rotated such that the antennas project normal to the 6U faces of the satellite would fit the form factor of the satellite quite well.

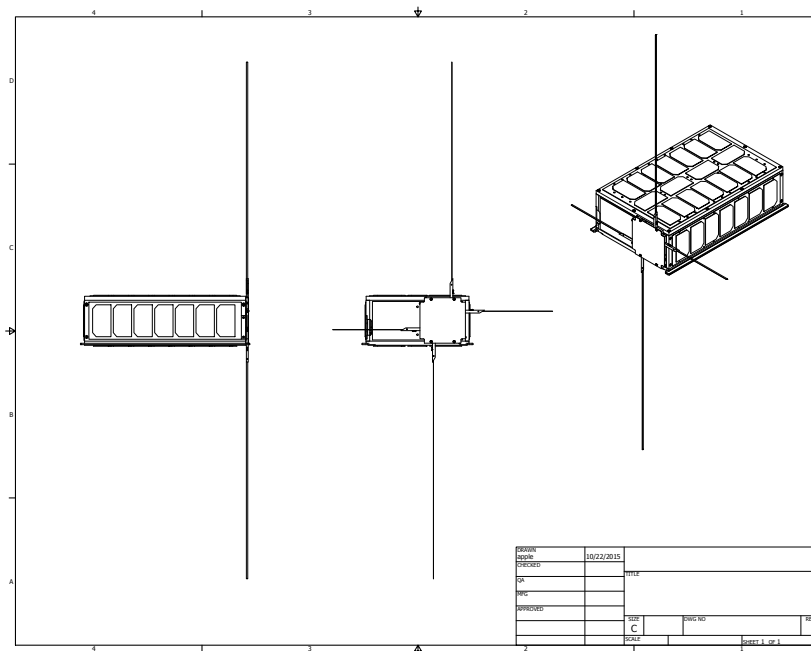


Figure 4.13: ISIS Quad monopole turnstile antenna on 2U face opposite the payload.

Given that either the single dipole or single monopole configuration could be chosen for RECONSO, the radiation patterns of each option are presented below in Figures 4.14 and 4.15. The radiation patterns shown are the ideal case for a 2U or 3U CubeSat form factor. A 6U simulation is not included as ISIS does not make the results of those simulations available on their website. It is assumed that the radiation pattern will be slightly damped along the longitudinal axis of the field due to the presence of the larger structure. Both of these radiation patterns are consistent with the planned pointing of the maximum gain towards the ground station during each pass as stated by the RECONSO Concept of Operations (CONOPS).

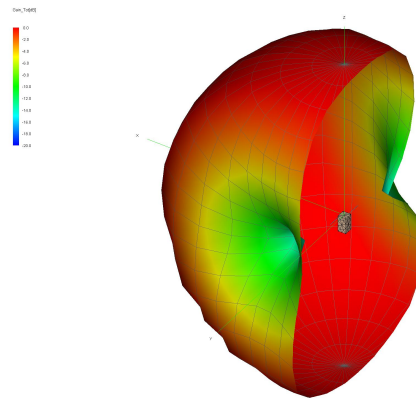


Figure 4.14: Radiation pattern of the ISIS Monopole antenna on a 2U CubeSat contoured from -20 dBi to 0 dBi

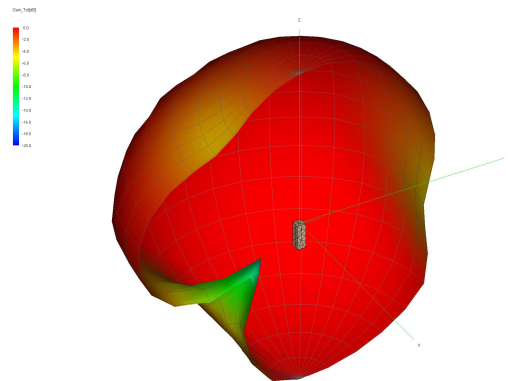


Figure 4.15: Radiation pattern of the ISIS Monopole antenna on a 3U CubeSat bus contoured from -20 dBi to 0 dBi.

The next option that will be structurally examined is the GOMspace AT430 UHF Turn-stile Antenna. Unlike the ISIS option that stores the antenna within the structure of the component before deploying outwards via a burn-wire, this option consists of 4 monopole antennas that extend radially from the face of the satellite. Instead of being stored within the component, the antennas are laid flush to the adjacent faces of the satellite. This option presents advantages in the gain that it provides, but difficulties in structural mounting. The stowed structural mounting is presented in Figure 4.16 and the deployed structural mounting is presented in Figure 4.17. The ideal radiation pattern for a 3U CubeSat bus is presented in Figure 4.18. Again, the 3U radiation pattern is the only available simulation for this component and is assumed to be similar to the 6U case.

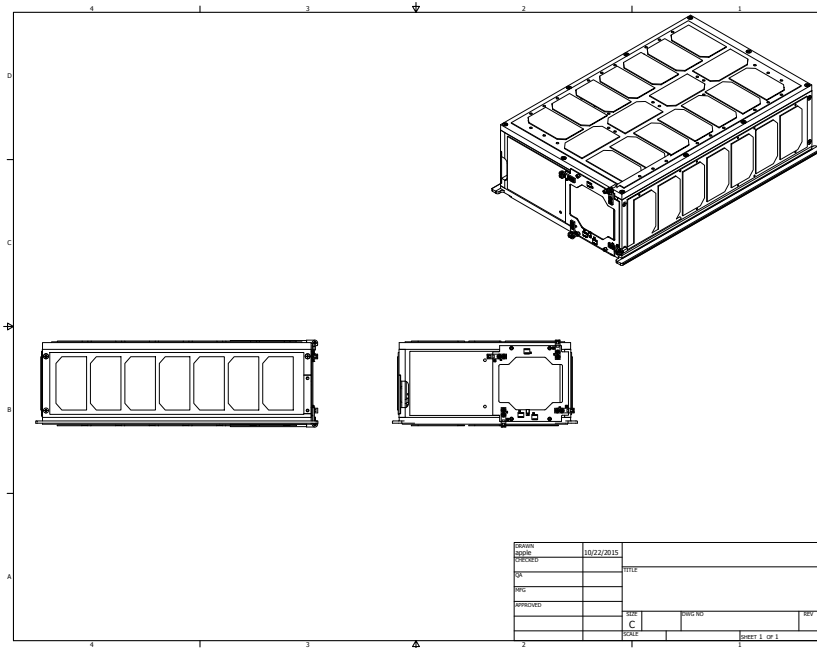


Figure 4.16: Depiction of the stowed GOMspace AT430 antenna mounted on the 2U face opposite the optical train.

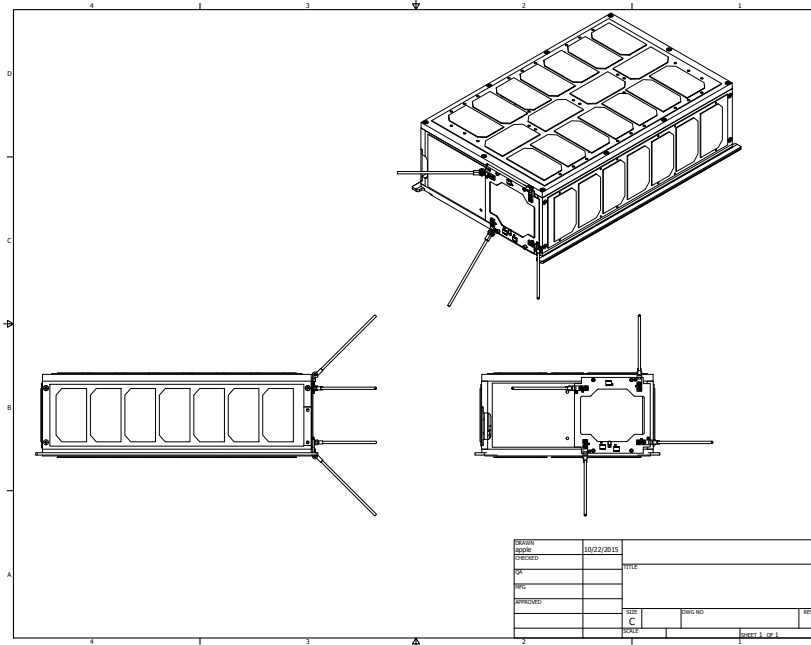


Figure 4.17: Depiction of the deployed GOMspace AT430 antenna mounted on the 2U face opposite the optical train.

It can be seen that the antennas stowed against the 2U surface will have to be modified so that they can lay at a 180° angle to the face of the antenna module rather than their designed 270° angle. Additionally, it will be difficult to modify the component such that the antennas lying flush to the 6U surfaces of the satellite will not interfere with the solar cells.

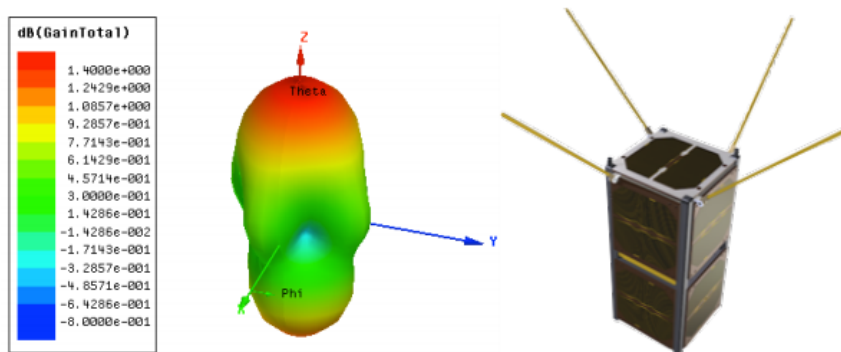


Figure 4.18: Radiation pattern of the GOMspace AT430 antenna contoured from -0.8 dBi to 4 dBi. This option exhibits higher gain and higher directionality than the ISIS option.

The radiation pattern of the GOMspace AT430 exhibits higher gain than that of the ISIS antenna, but is much more direct. Given that the RECONSO satellite will not have very fine pointing requirements, a broader high-gain pointing area is desired over a narrower but higher-gain pointing area.

An antenna constructed in-house from a tape measure offers a very cheap alternative to the aforementioned components. This option has been flown on numerous missions before and is as seen as feasible method of constructing an antenna that will reliably deploy as soon as the satellite is ejected from its deployer. A mounting apparatus typical of a tape measure UHF antenna is shown below in Figure 4.19 and such a component integrated with a complete satellite is shown in Figure 4.20.



Figure 4.19: A mounting apparatus typical of a tape measure UHF antenna.



Figure 4.20: The tape measure antenna shown on the flight-ready Finnish Aalto-1 satellite.

The tape measure antenna passively deploys due to the stored stress of a tape measure that has been folded over its short axis. This is an advantage over the active deployment via burn-wire that the other two options require. The most effective use of a tape measure antenna on the RECONSO satellite would be folding a dipole or dual monopole antenna normal to the 6U faces of the satellite. This would allow for the area of highest gain to be pointed directly opposite the drive train so as to not interfere with the exclusion zone of the pointing requirements. An advantage of this option is that the length of this antenna could be adjusted so as to be precisely the right length for the frequency to which the RECONSO satellite is assigned while on-orbit. The design and use of this antenna, however, requires a very in-depth understanding of radio communication and antenna design. It also requires manufacturing a component in-house that is very critical to mission success.

As far as the mass budget is concerned, each of the options considered in this section all weigh under 100 grams and would all require the same, low-mass harnessing connecting

the antenna to the UHF daughterboard on the Tyvak Intrepid flight computer. As such, mass is a non-issue with all of these options. Additionally, all of these options can operate in a much wider range of thermal conditions than the rest of the spacecraft, making thermal considerations a non-issue as well.

Based on the analysis presented here, the ISIS dipole antenna and the tape measure antenna are structurally favorable over the GOMspace AE430 antenna.

Impacts on EPS

The electrical considerations for each of these antenna options are the maximum gain that an antenna provides and the max RF power that it is capable of broadcasting. This is an area where the ISIS and GOMspace options present significantly less risk than the tape measure option. While the tape measure may be more customizable to the RECONSO satellite, it will require much more testing and characterization to fully understand the performance of the antenna.

The gain, max RF power, and operating voltage of each antenna option are presented below in Table 4.13.

Table 4.13: Technical specifications of UHF antenna options

	ISIS Dipole	GOMspace AT430	Tape Measure
Gain	0 dBi to -20 dBi	1.5 dBi to -1dBi	Unknown
Max RF Power	2 W	10 W	Unknown
Operating Voltage	3.3 V or 5 V	5 V	Customizable

Based on these characteristics, it is concluded that the ISIS Dipole and GOMspace AT430 antennas are electrically favorable to the tape measure antenna. The difficulty in characterizing the tape measure antenna presents mission risk that is not present in the other two options.

Impacts on CDH

Each option presented has various effects on the CDH subsystem. All options will require a single feedline from the flight computer to the antenna. However, the ISIS Dipole antenna will also send safe/arm status, deployment status, and temperature telemetry via an I²C connection to the flight computer. This makes the ISIS Dipole antenna slightly preferable to the other two options from a CDH perspective.

Impacts on MGT

The MGT concerns with the antenna trade are threefold: cost to acquire a component, time to acquire a component, and reliability of a component. Reliability of a component and time to acquire said component represent much more significant project risk than monetary expense. Given the integral nature of the COM system with the primary mission functionality of the satellite, a COM system with extensive flight heritage is preferable to one that

has never been flown before. In terms of schedule risk, previous efforts at the integration of the COM system have been completely stalled due to the time delay in acquiring S-Band components from Astrodev LLC. MGT preference will be given to the option that is believed to be the most reliable and can still be acquired in a reasonable timeframe. The managerial characteristics of each option are presented in Table 4.14.

Table 4.14: Management risks of UHF antenna options

	ISIS Dipole	GOMspace AT430	Tape Measure
Cost	\$5090	\$6220	less than \$250
Schedule Risk	8-12 weeks	6-10 weeks	est. 8 weeks required for antenna design
Flight Heritage	High	High	Low

In terms of managerial preferences, the ISIS Dipole and GOMspace AT430 are very similar options.

Conclusion

Based on the results presented in this section of the trade study, the ISIS Dipole antenna is chosen as the ideal option. The effects of this choice on each subsystem examined are shown below in Table 4.15. Each option is assigned a point value 1-3 for each subsystem, with the winner being the option with the most points.

Table 4.15: UHF antenna trade evaluation

	ISIS Dipole	GOMspace AT430	Tape Measure
STR	3	1	2
EPS	2	3	1
CDH	2	1	1
MGT	2	2	1
Total	9	7	5

4.2.3 Evaluation of Downlink System

The downlink system of the satellite will be chosen based on reliability of the system, data rates possible, and compatibility with the existing satellite. There are 3 options available for the downlink capabilities of the RECONSO satellite:

1. S-Band
2. GlobalStar Simplex
3. GlobalStar Duplex

The existing COM system is baselined on the use of UHF uplink and S-Band downlink. The current S-Band component options have been abandoned due to a lack of communication from the manufacturer, Astrodev LLC. Should S-Band be used for downlink, it is assumed that the existing UHF system would be used for uplink. If the GlobalStar Simplex is used for downlink, the existing UHF system would also still be used for uplink. However, if the GlobalStar Duplex is chosen for downlink, it would also be capable of uplink capabilities. This would give the COM system a level of redundancy not found with the other 2 options. The UHF system could then be configured for entirely backup COMs or a beacon, providing more confidence of mission success and a much higher fault tolerance than would otherwise be available.

In following the traditional RECONSO design paradigm, flight tested components from reliable manufacturers will be most strongly considered. The following S-Band systems will be examined:

1. ClydeSpace CubeSat S-Band Transmitter¹⁸ with the ClydeSpace S-Band Patch Antenna¹⁹
2. ISIS TXS S-Band Transmitter²⁰ with the Clyde-Space S-Band Patch Antenna²¹
3. ISIS HISPICO S-Band Transmitter²² with the ISIS HISPICO S-Band Patch Antenna²³

All of these components are designed to fit with the nominal 1U stack, and so it is not anticipated that there will be any problem with fitting them into the structure of the satellite. As for the mounting of the antenna, there are two options available. Given the placement of the UHF antenna, the only other options are next to the UHF antenna or next to the boresight of the camera.

Impacts on STR

All of the aforementioned S-Band systems could fit on the existing structure of the RECONSO CubeSat. However, the GlobalStar system and S-Band system offer different options for power generation and antenna placement. Given that the S-Band system will need to be communicating with a ground station on the Earth, the patch antenna will need to be pointed at the ground station to ensure optimal COM operation. However, given that the GlobalStar system will be communicating with a constellation of other satellites, it will have much less strict pointing requirements. It would actually be detrimental to the performance of the GlobalStar system to have the antenna pointed at the ground. There are therefore two options. These two options are shown below in Figure 4.21.

¹⁸Clyde-space.com; accessed 3/30/2017

¹⁹Clyde-space.com; accessed 3/30/2017

²⁰cubesatshop.com; accessed 3/30/2017

²¹Clyde-space.com; accessed 3/30/2017

²²cubesatshop.com; accessed 3/30/2017

²³cubesatshop.com; accessed 3/30/2017

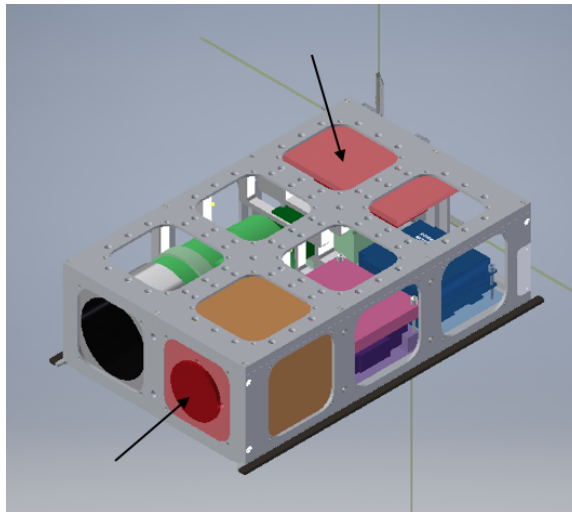


Figure 4.22: Placement of the GlobalStar Duplex board integrated with the satellite internals. The GlobalStar board and patch antenna are emphasized with arrows.

Impacts on CDH

As far as CDH is concerned, there is much more documented history of the GlobalStar Duplex working in tandem with the Tyvak Intrepid flight computer than there is with the Simplex. The wiring for the Tyvak Intrepid to the GlobalStar board along with documentation on the necessary connections for the Duplex board is presented below in Figure 4.23.

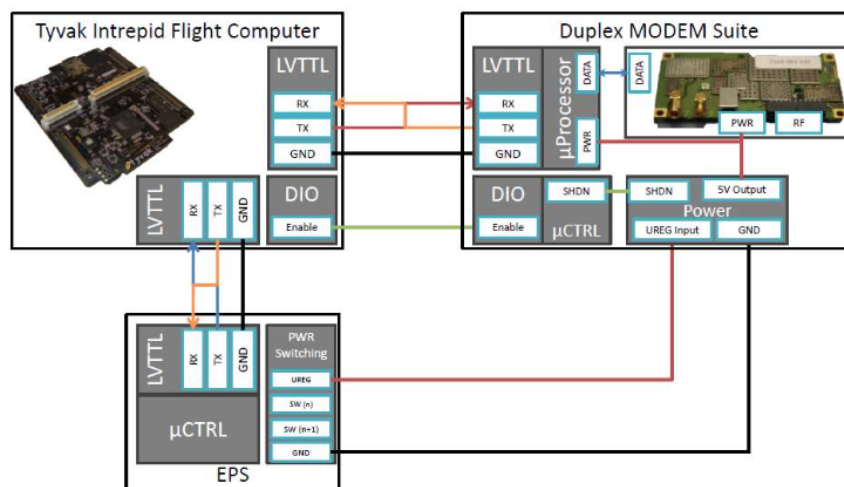


Figure 4.23: Wiring documentation of the Duplex MODEM Suite and Tyvak Intrepid.

While not incredibly comprehensive, the information available regarding the use of the Duplex module in conjunction with the Tyvak Intrepid is slightly more favorable than that of the Simplex.

Impacts on MGT

The biggest advantage that the GlobalStar Duplex offers over the Simplex or S-Band systems is in the area of mission risk. Being a flight tested system, the GlobalStar system offers much more dependability for very similar schedule and budgetary costs than a comparable S-Band system. Additionally, the use of the GlobalStar Duplex system offers alternatives for primary and secondary COM systems not available with the other choices.

With the GlobalStar Duplex as a primary COM system, the UHF system on the spacecraft can be used almost entirely as a backup COM system. While the GlobalStar Duplex can function for primary mission functionality, the UHF system can be used as a beacon during various health modes of the satellite such that the Georgia Tech ground station can be used to verify the health of the satellite without having to command the downlink of telemetry or health data. The UHF system can also be configured for both uplink and downlink to command the satellite should the GlobalStar option not be available. For mission data, the much more frequency access that the GlobalStar Duplex offers is much preferable to the ground station passes that the other systems would have to accommodate for.

In terms of budget, the only downside of the GlobalStar Duplex is the cost of data. Currently, there are approximately \$40,000 budgeted for the cost of data. The cost of data according to NearSpace Launch is presented below in Table 4.16.

Table 4.16: NearSpace Launch cost of GlobalStar Duplex operation

Connection Duration (min)	Approx. throughput (MB)	Rate (\$/min)	Cost Range (\$)
1-10	0.04 - 0.42	0.85	0.85 - 8.50
11-100	0.421 - 4.2	0.6375	7.01 - 63.75
101-1000	4.21 - 42	.425	42.39 - 425.00
1001-10000	42.01 - 420	0.3825	382.88 - 3825.00
10001+	421.01+	0.34	3400.34+

Assuming that the mission operations requires a maximum of 1GB of data throughput each month, the cost of the GlobalStar Duplex data should not be an issue for a 6 month nominal mission lifetime. Given that the data downlinked by RECONSO will have actionable value to both the public and private sector, it is very likely that data costs could also be picked up by another party for extended mission life.

Conclusion

The GlobalStar Duplex system will be used for primary COM uplink and downlink due to its reliability, compatibility with the CONOPS, and ease of operation compared to traditional CubeSat COM systems. The UHF system will be used as a redundant COM system for uplink and downlink and will be used as a beacon during high power safe modes. The cost of this system will not be an issue. The below image summarizes these decisions of and demonstrates how the satellite will interact with the ground station over the primary and secondary COM channels.

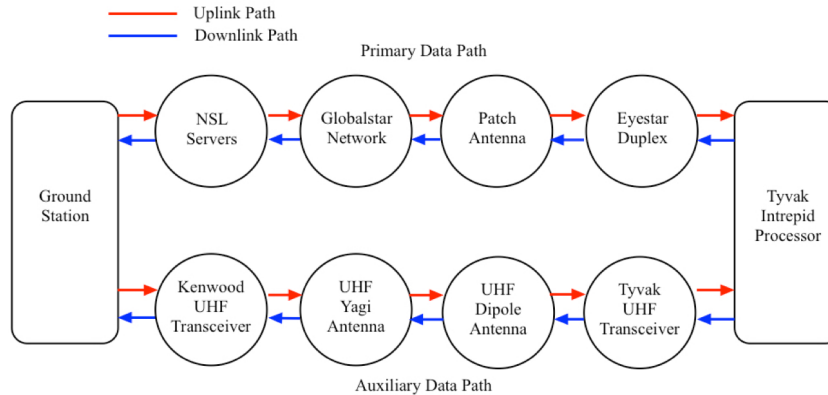


Figure 4.24: Summary of Uplink/Downlink systems through primary and secondary channels

4.2.4 Evaluation of Ground Station

The ground station that will be used by the RECONSO mission will also be used by the PROX-1 mission. Given that the PROX-1 mission is a more mature flight project than RECONSO, many of their ground station design changes take priority over those made by the RECONSO mission. Additionally, assuming the PROX-1 mission launches on schedule, the PROX-1 team will be conducting on-orbit operations during the spring 2018 semester.

The three characteristics of the ground station that are desirable to the RECONSO mission are as follows: effective use for our satellite, ease of access for testing, and ease of customization. Sharing facilities entirely with the PROX-1 mission is contrary to these objectives, and so the RECONSO mission must divorce its ground station functionality from that of the PROX-1 mission. PROX-1 has recently decided to move the Georgia Tech S-Band equipment to an off-campus location that is outside of Atlanta. This offers them a broader horizon that is free of many of the large buildings that make the on-campus S-Band ground station undesirable. This increase in distance also makes testing of flight hardware by mission personnel logistically more difficult and requires a maturity of hardware that RECONSO does not currently have given the on-campus clean room where the satellite will be located for testing. The options available to the RECONSO mission at this junction are as follows:

1. Share UHF and S-Band facilities
2. Share only UHF facilities
3. Share no facilities

The consideration of S-Band facilities is not essential to this trade given the outcome of the previous trade regarding the downlink functionality of the satellite removing the S-Band system from the satellite. However, the use of S-Band facilities is still evaluated due to the opening conditions of this trade requiring its examination. This trade does not heavily impact the technical areas of the project, so only managerial aspects of the trade are taken into account.

Impacts on MGT

There are a number of requirements that are imposed on the management of the RECONSO mission that have been enumerated below.

1. Do not interfere with mission-critical testing of the PROX-1 satellite
2. Do not interfere with on-orbit operations of the PROX-1 satellite
3. Adequately test the RECONSO satellite
4. Do not needlessly buy new equipment

The first two of these requirements necessitates at least some separation of the RECONSO and PROX-1 ground stations. In order for both projects to get done what they need to do, the same facilities cannot be used by both groups. However, the question still stands as to whether or not the purchase of an entire new ground station is necessary. The construction of an entirely new ground station on the roof of the Howey Physics building would come at a cost of approximately \$15,000 to the RECONSO project. The construction of a new S-Band system on the roof of the Montgomery Knight building would also be a large expense. These needlessly large expenses would be irresponsible and frivolous. In order to test the RECONSO satellite effectively and while still responsibly managing the RECONSO budget, the existing Montgomery Knight ground station should be used to the fullest extent possible without interfering with the PROX-1 mission.

Conclusion

Given the aforementioned requirements and analysis, the following actions will be taken by the RECONSO mission:

1. Purchase a cheap monopole antenna for use by the RECONSO mission for testing in the Montgomery Knight ground station
2. Repurpose an extra computer and TNC for use by the RECONSO COM subsystem

The use of a monopole antenna located inside the building has negligible difference to a large antenna placed on the roof of the building when the satellite is a mere 100 feet away. As such, the majority of the COM subsystem testing can be carried out with equipment that belongs entirely to the RECONSO mission. PROX-1 and RECONSO on-orbit operations will not be taking place at the same time, so the two projects will never have to worry about using the Yagi UHF antenna at the same time and much conflict will be avoided.

4.2.5 Trade Conclusion and Summary

1. UHF antenna will be the ISIS Dipole antenna. UHF will be used as uplink and downlink as well as a beacon during high power safe mode.
2. Downlink system will be the GlobalStar Duplex. This will also function as the primary uplink system.
3. Ground station hardware will be divorced from mission-critical PROX-1 hardware.

4.3 CONOPS

Having closed these two major trades, the final aspect of the mission that needs to be closed is the CONOPS. While the CONOPS can be defined in terms of mathematical terms for payload and system sizing and design, it must be defined in terms of duty cycles, subsystem requirements, and hardware limitations in order to carry out engineering of the system. The CONOPS are summarized in this section.

4.3.1 Overview of RECONSO hardware and software

Nominally, the RECONSO mission is accomplished by a camera and lens that take pictures of space objects as they pass across the field of view of the satellite. However, there are many other peripheral pieces of hardware and software that are required to operate this payload on-orbit. The table below reflects each of the pieces of hardware that will be flown on RECONSO. The Structures subsystem is not reflected in this table as it is assumed that their hardware will not be actively cycled or deployed as part of the CONOPS.

It should be noted that there are three different computers that are being flown on the RECONSO CubeSat. Their functions may be summarized as follows: The Tyvak Intrepid will run all FSW architecture and communications with the ground station. The Innoflight CFC-300 will be connected to the payload camera and will handle all image processing and payload operations. The BeagleBone Black (BBB) will be connected to all ADCS hardware and will handle attitude determination and control implementation.

The main blocks of RECONSO software are reflected in the following table. cFE allows for the packaging of various pieces of code as individual apps that run within the framework of cFE. Some of these apps come built into cFE, while others will be written by the RECONSO team to allow for more mission-specific functionality than what cFE is able to provide. It should be noted that there are also many pieces of software that are built into each one of these pieces of hardware by the manufacturers to allow it to function as intended.

4.3.2 Overview of Flight Software

In the interest of clarifying the nomenclature of the RECONSO FSW team from those used by other groups that are employing the cFE architecture as well, the purpose of each block of FSW will be briefly explained. Please note that this is not being done from a computer science perspective, but rather from a systems-engineering perspective, with the interest of being easy to understand by those without a background in computer science. the reader should refer back to this list throughout the document to aid in the understand of how each piece of software will help accomplish the goal of each mode of the satellite.

1. Image Processing - When analyzing pictures taken by the payload, this block of code will handle the opening and reading of each image file.
2. Star Tracker - While taking pictures, the star tracker will compute angular distance between stars in each picture and compare them to an on-board star catalog to precisely determine the attitude of the spacecraft. This code will run in real time with a frequency of 10 Hz.

Table 4.17: All components of RECONSO flight hardware and software.

Subsystem	Hardware
PAY	Kowa LM60JS5MA Lens
PAY	Nocturn XL CMOS Camera
PAY	Innoflight CFC-300 Processor
EPS	ClydeSpace 30Wr Battery
EPS	ClydeSpace PMAD Distribution board
EPS	In-house EPS Breakout board
EPS	In-house Inhibit board
EPS	In-house Solar panels
ADCS	Analog Devices Inertial Measurement Unit
ADCS	Pumpkin GPSRM 1 GPS Receiver
ADCS	AntCom 1.5G L1 GPS Antenna
ADCS	In-house sun sensors
ADCS	In-house magnetorquers
ADCS	Tyvak Magnetometer
ADCS	BBB ADCS Controller
COM	Tyvak UHF Daughterboard
COM	ISIS UHF Dipole Antenna
COM	NSL GlobalStar Duplex
COM	NSL GlobalStar Patch Antenna
TCS	Omega Resistive Temperature Detector
TCS	Omega 10 Whr Heater
TCS	In-house thermal board
CDH	Tyvak Intrepid
CDH	In-house CDH Breakout board

Software	Processor
Image Processing	CFC-300
Star Tracker	CFC-300
Star Subtraction	CFC-300
Object Tracking	CFC-300
ADCS Controller	BBB
ADCS Hardware polling	BBB
Health Monitoring	Tyvak Intrepid
EPS Hardware Controller	Tyvak Intrepid
TCS Hardware Controller	Tyvak Intrepid
Innoflight CFC-300 Hardware Controller	Tyvak Intrepid
BBB Hardware Controller	Tyvak Intrepid
Finite State Machine (FSM)	Tyvak Intrepid
Scheduler	Tyvak Intrepid
File Manager	Tyvak Intrepid
Message Bus	Tyvak Intrepid
Event Log	Tyvak Intrepid
UHF COM Receive	Tyvak Intrepid
UHF COM Transmit	Tyvak Intrepid
GlobalStar COM Receive	Tyvak Intrepid
GlobalStar COM Transmit	Tyvak Intrepid

3. Star Subtraction - While analyzing pictures to track objects, the star subtraction code will determine which features of the image are stars and remove them from subsequent frames so that they are not tracked as objects.
4. Object Tracking - After the stars in a given image have been subtracted, the object tracking code will track objects in subsequent frames to determine their right ascension and declination relative to the spacecraft as well as their photometric brightness.
5. ADCS Controller - The ADCS controller will analyze measurements taken from each ADCS sensor, take into account each sensor's known uncertainty, and filter this data to determine what action should be taken by the actuators to reach a desired attitude.
6. ADCS Hardware Polling - ADCS hardware polling regards the use of serial com-

munications protocol to request data from each ADCS sensor at a frequency of 10 Hz.

7. Health Monitoring - To ensure that the spacecraft is operating nominally, the health monitoring software will poll various sensors in various subsystems of the spacecraft and compare it to safe values.
8. EPS Hardware Controller - The EPS hardware controller will be used to communicate with the EPS stack to determine which components are receiving power at a given time and how much power they are receiving.
9. TCS Hardware Controller - The TCS hardware controller will poll the thermal board's resistive temperature detectors (RTDs) and heaters to determine the thermal state of the spacecraft and whether or not heaters or components need to be turned on or off.
10. Innoflight CFC-300 Hardware Controller - The Innoflight controller will be used to handle all serial communication when polling payload data from the Innoflight CFC-300. All object tracks and stars in the field of view will be stored locally on the CFC-300 and will be sent to the ADCS Controller as it is requested.
11. BBB Hardware Controller - The BBB controller will handle serial communication between the primary flight computer and the BBB. While the ADCS controller makes attitude determinations, the hardware controller will allow pointing commands and desired attitude of the spacecraft to be passed to the BBB.
12. Finite State Machine - The FSM will receive health data and determine the correct mode of operations for the satellite at any given time. Should a mode switch be necessary, the FSM will determine what pieces of hardware need to be turned on or off and what software processes need to be started or stopped.
13. Scheduler - The scheduler will control when various software apps run so that processes are not started or stopped in the incorrect order. It can be considered to be a timetable of events through which the satellite moves in chronological order.
14. File Manager - When a process needs to retrieve the contents of a memory address on board the spacecraft, the file manager will return those contents to the process that requests them. When a process needs to store a file, the file manager will write the contents of that file to memory and return their memory address.
15. Message Bus - The message bus serves as the communication path along which every process can pass messages to every other process running onboard.
16. Event Log - The event log will be used to recording software events as they happen along with a timestamp. This will be used for the ground to debug any software errors and to ensure nominal function of the satellite.
17. UHF COM Receive - The UHF COM Receive app communicates with the UHF Daughterboard to receive and pass along the message bus any messages that the satellite receives from the ground over UHF.

18. UHF COM Transmit - The UHF COM Transmit app communicates with the UHF Daughterboard to package messages that the satellite sends to the ground over UHF.
19. GlobalStar COM Receive - The GlobalStar COM Receive app serves the same purpose as the UHF COM Receive app, except it communicates with the GlobalStar Duplex.
20. GlobalStar COM Transmit -The GlobalStar COM Receive app serves the same purpose as the UHF COM Transmit app, except it communicates with the GlobalStar Duplex.

4.3.3 Spacecraft Modes of Operation

As was mentioned in the previous section, the mode switching on RECONSO will be handled by the FSM built-in cFE application. The FSM application will command various components and processes to either begin or end operations based on the mode into which it determines the satellite currently needs to operate.

The FSM will make these decisions based off of health data, commands in the scheduler, and the location of the satellite in its orbit. At a basic level, the decisions that the FSM will step through are portrayed in the two images below.

Figure 4.25: Operation of RECONSO over the course of the entire mission lifetime.

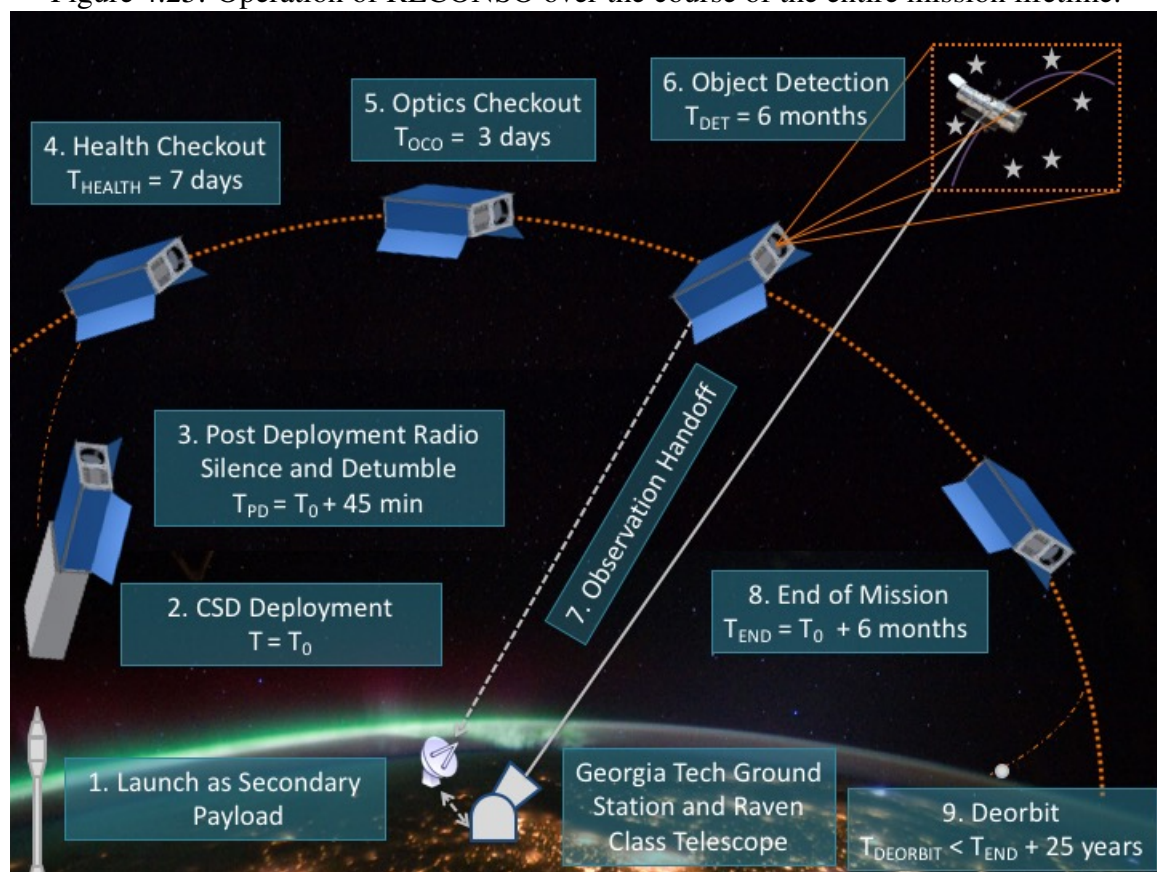
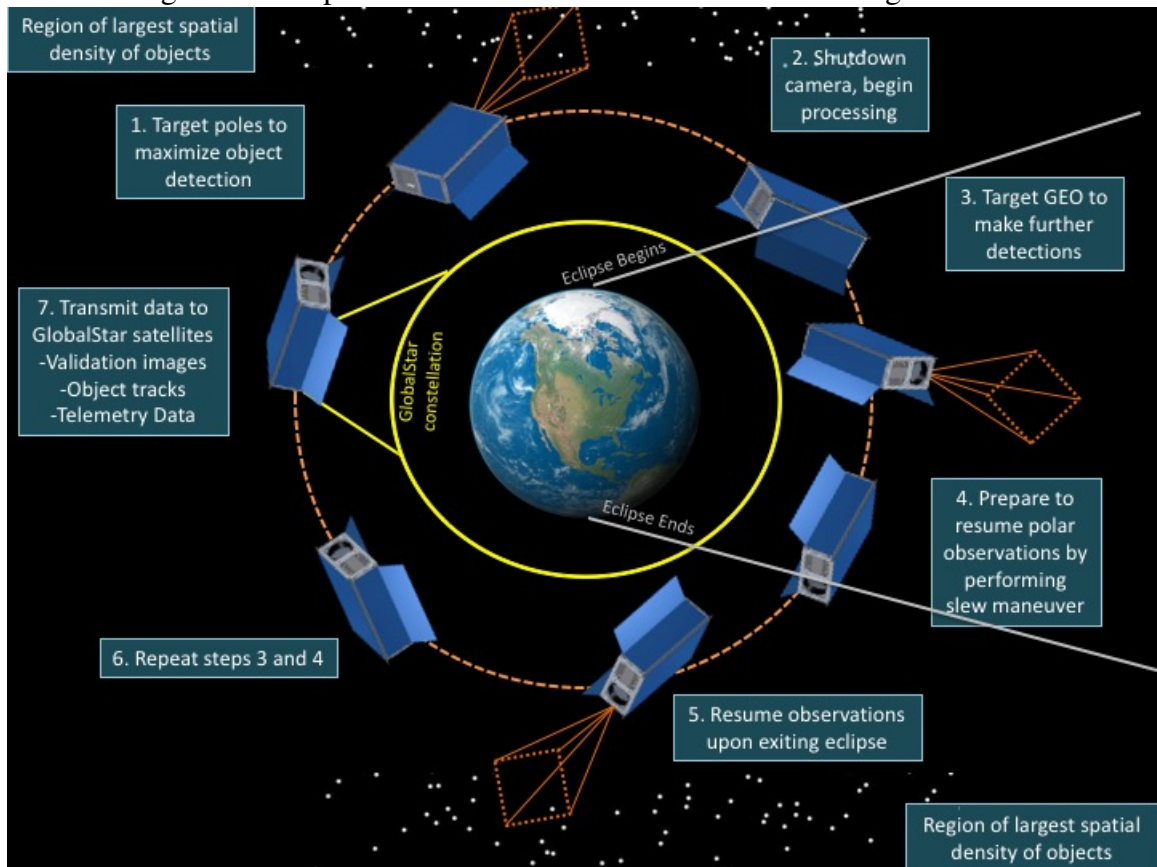


Figure 4.26: Operation of RECONSO over the course of a given orbit.



In order to accomplish these operations, the satellite will have several modes of operation between which it will switch. The remainder of this document will be dedicated to addressing each of these modes in detail. The overview, entry criteria, exit criteria, operational hardware, and operational software of each mode will be described, along with any additional pertinent information that goes with each mode.

Before beginning, it should be noted that there are certain pieces of hardware and software that will always be used, throughout all modes of spacecraft operation. In the interest of avoiding repetitiveness, these items will be outlined in the table below. They will not be included in the tables defining the operational hardware and software in subsequent mode definitions.

It should be noted that the only items operational throughout all modes is only that hardware necessary to the integrity of the spacecraft. The EPS subsystem will always be conducting operations that help determine the health and basic functionality of the satellite. At its most basic state, the batteries will be used to determine that an unacceptable depth of discharge has been reached and only the bare minimum hardware and software will be run until the batteries can be replenished through power output from the solar panels.

Each of the modes will list only hardware and software items that will be used in addition to these items.

Table 4.18: Operational components of the RECONSO system throughout all modes.

Subsystem	Hardware	Software	Processor
EPS	ClydeSpace 30Whr Battery	Health Monitoring	Tyvak Intrepid
EPS	ClydeSpace PMAD Distribution board	EPS Hardware Controller	Tyvak Intrepid
EPS	In-house EPS Breakout board	Finite State Machine (FSM)	Tyvak Intrepid
EPS	In-house Inhibit board	Scheduler	Tyvak Intrepid
EPS	In-house Solar panels	File Manager	Tyvak Intrepid
CDH	Tyvak Intrepid	Message Bus	Tyvak Intrepid
CDH	In-house CDH Breakout board	Event Log	Tyvak Intrepid
		UHF COM Receive	Tyvak Intrepid
		GlobalStar COM Receive	Tyvak Intrepid

CHAPTER 5 CONCLUSION

This paper has covered the entire development of the RECONSO CubeSat to date. The mission profile of RECONSO was formulated as a given observer with known position and attitude dynamics detecting a space object at unknown distance and direction with unknown position and attitude dynamics. Various constraints were placed on the system such that the detectable region of space objects could be fully bounded and predictions of system performance could be made using the existing space object catalog. Assumptions were made such that the performance of the system could be defined in terms of the number of space objects detected by a real observer with the modern state-of-the-art payload hardware. This allowed for further driving assumptions to be made regarding mission requirements, hardware selection, and satellite development. The selection and hardware and mission requirements drove the design of the concept of operations of the satellite, which was initially defined in a purely theoretical sense, into something that could be accomplished with hardware, budget, and development constraints. The RECONSO CubeSat and the student engineers that have been building it have made extraordinary progress towards creating a spacecraft that will affect the design paradigm for space surveillance and space object detection.

The RECONSO CubeSat has been under development since early 2013, when it was accepted as a proposal to the AFRL UNP 8. At the time of writing, it is expected that the satellite will ship to AFRL facilities for environmental testing in fall 2017 for a spring 2018 launch. All told, it satellite will have undergone a development cycle of approximately five years. That figure alone is not incredibly outstanding for a development lifecycle of a basic spacecraft, but the financials behind the development of RECONSO truly set it apart from the industry standard. The AFRL funding of \$220,000 has been combined with funding from the Georgia Institute of Technology and donations from various industry partners to total around \$250,000 before launch. The benefit of developing satellites in a university environment is clear in these figures. The labor for the project has been almost entirely donated through a majority workforce of undergraduate students who are attempting to develop fledgling engineering skills through working on a practical project and graduate students who are attempting to create impactful research and contribute meaningfully to their field. The time of the various professors and of our principal investigator, Dr. Holzinger, has also largely been donated. A development cost of 5 years and \$250,000 is rival to even the most cost-cutting privatized space companies.

Professors within academia are uniquely situated to see all aspects of the space community in ways that other players are not. The creation of a space-based space object detector has very little profit proposition for a privatized company unless under contract with the government. Those contracts that are under government provision are almost always subject to the mission profiles and restrictions of government benefit and, as such, are often classified or created in line with traditional aerospace paradigms of large enterprise-class missions with the associated long timelines and exorbitant costs. While still subject to

AFRL and thus US government mission profiles, the RECONSO CubeSat will cut neatly between these two worlds. While still subject to government and military interests through the oversight of AFRL, the substitution of education in lieu of pay has been able to cut cost relative to traditional government contracting models. Grant-based educational development of CubeSats and spacecraft in general enables the deployment of high quality space technology at very competitive rates and will continue to provide meaningful results through RECONSO and countless other projects for years to come.

Appendices

APPENDIX A UHF RADIATION PATTERN

Having selected the UHF antenna, the structure of the spacecraft can be roughly modeled and an electromagnetic analysis run to determine the radiation pattern that RECONSO will have for its downlink system. The two images below demonstrate a mock-up of the spacecraft structure as a 6U hollow block of aluminum with the grounding plane as the rear 2U panel and the two conducting elements being the same size and location of the ISIS Dipole antenna. It should be noted that this is only a preliminary analysis done for purposes of confirmation of trade study results and that a CAD model of the entire spacecraft will be used in later simulation and analysis.

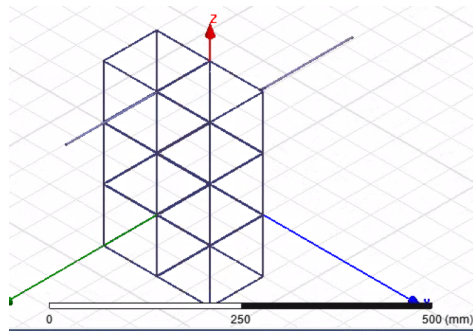


Figure A.1: Mock-up of the RECONSO 6U structure

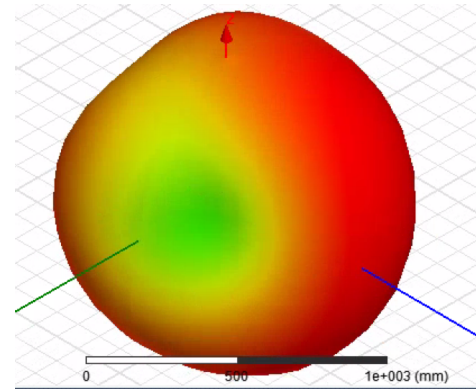


Figure A.2: Resultant radiation pattern on UHF for the ISIS Dipole antenna

These results are approximately what would be expected out of the dipole configuration. There are no sections of the radiation pattern that demonstrate severe loss and there is a wide area of acceptably high gain reception to allow for uplink and downlink over the UHF system as secondary COM. This is also good because, as a secondary COM, it is likely that UHF would only be used for primary communication with the spacecraft during times when the spacecraft is otherwise unresponsive over the primary COM system. If the primary COM system were to be inactive, it would be much more possible that the spacecraft would have lost attitude control or otherwise be experiencing general system anomalies. As such, it is good that the UHF system has a wide area of acceptable gain such that UHF COM can be used even without having fine pointing control over the spacecraft.

APPENDIX B LINK BUDGET ANALYSIS

The link budget must be included as an aspect of this trade study in order to fully understand whether or not the system will be capable of accomplishing subsystem requirements that flow down from mission success criteria. Assuming an averaged radiation pattern, which Appendix A shows is a mostly valid assumption, the average gain from the system can be calculated using the ITU's satellite link budget analysis worksheet. Given that RECONSO does not yet have a specified launch slot and orbit, the gain was calculated at various altitudes assuming that the satellite would be talking to the Georgia Tech ground station in Atlanta, GA over UHF (137 MHz). COM has a subsystem requirement of 6 dB for uplink and downlink to meet success criteria.

Orbital Altitude	Uplink Margin
300 km	30.5 dB
800 km	19.4 dB
1200 km	16.8 dB
Orbital Altitude	Downlink Margin
300 km	6.9 dB
800 km	0.1 dB
1200 km	-2.6 dB

Figure B.1: UHF gain calculated at various orbital altitudes

It can be seen that for the UHF system, uplink will close the subsystem requirements regardless of the orbit that the spacecraft is placed into. The downlink, however, is much more contingent on a lower orbit than the uplink is. While this system may not meet minimum mission requirements, it should be noted that it is not necessarily required that the UHF (backup) system meet these requirements. UHF will only be used in the event that the GlobalStar system becomes unavailable, and thus only needs to allow for commanding of the satellite while the satellite or the GlobalStar system may be temporarily unresponsive.

A link budget analysis of the GlobalStar system is much more difficult to carry out than the link budget analysis of the UHF system is. Given that there does not yet exist sufficient documentation or testing to fully quantify the throughput of the GlobalStar system, it must instead be characterized in terms of various deficiencies that are known to be endemic to the system. The most important of these deficiencies is the high latency known to be involved with GlobalStar communications. This would be a severe detriment to the system if the satellite were to lose attitude control, preventing a sufficient link from being established between the RECONSO satellite and the GlobalStar constellation.

However, various assumptions can be made that allow for the risk of the system to be characterized based on the minimum mission success requirements of RECONSO.

1. Health telemetry must be downlinked for 1 week to perform health checkout
2. 1 payload image must be downlinked to perform optics checkout
3. 1 set of right ascension, declination, and photometric brightness of a space object track must be downlinked

Assuming each packet of health monitoring data amounts to approximately 500 bytes of IPv4-encoded data and that health telemetry will be sent through GlobalStar every hour for one week, there will be 84 kB of health telemetry data for one week of health checkout. The payload Nocturn XL camera will be taking images of 1280 x 1024 pixels, resulting in a file size of 1.3 MB per image taken. Assuming a lossless compression ratio of 1:2, each image downlinked will have an approximate file size of 650 kB. However, to be sure that everything works properly, it would be wise to downlink 3 images for optics checkouts, resulting in 1.95 MB of optics checkouts data. The ordered pairs of payload data for tracks developed will result in a text-only file that is approximately 5 kB large.

Assuming that it takes another 2 weeks of nominal operations before object detection begins in earnest and that only positive tracks are downlinked through the GlobalStar system, this results in approximately 3 MB of data (including generous margin) that needs to be sent through the GlobalStar system. Given the cost analysis presented in Table 7, this would incur a cost of approximately \$50 and would require a total connection duration of about 80 minutes. This would require 3 weeks of stable, attitude-controlled operations of the satellite and a pseudo-worldwide coverage of the GlobalStar constellation. The RECONSO mission is confident that the attitude control of the spacecraft will allow for this to happen with very high certainty. Every component on-board the spacecraft is designed to a nominal 6 month mission lifetime, so components have a very high probability of lasting for less than one month.

Thus, while not knowing the specifics of data throughput or latency of the GlobalStar system, the RECONSO mission can say with a high degree of certainty that the link budget will close completely on the GlobalStar system.

APPENDIX C MODE SWITCHING FLOW CHART

Note: This image is best viewed in a digital format, where the reader can zoom in on any desired section of the flow chart.

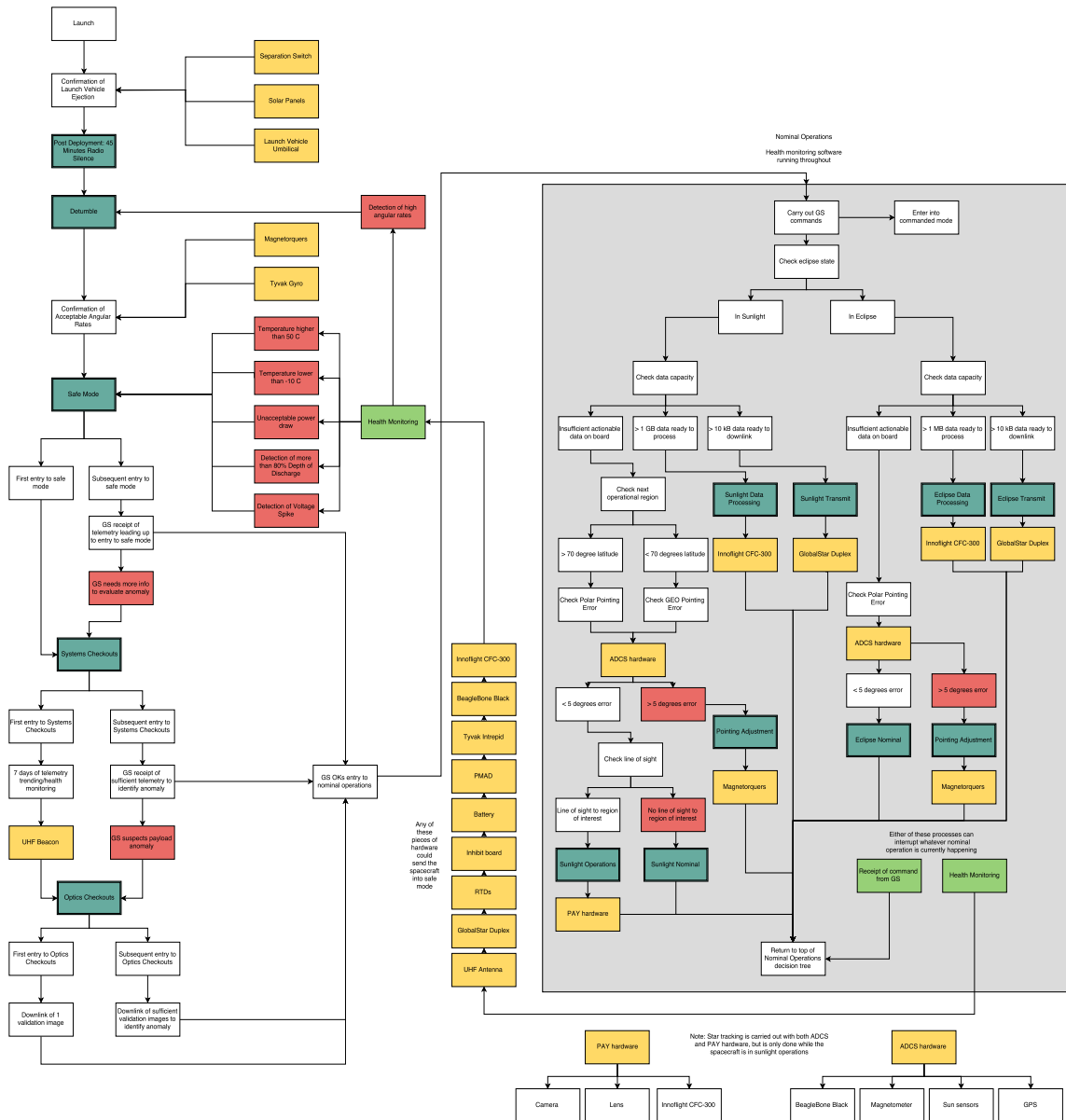


Figure C.1: Flight software CONOPS flow chart

BIBLIOGRAPHY

- [1] National Aeronautics and Space Administration. “Small Spacecraft Technology State of the Art”. In: *NASA/TP-2015-216648/REV1* (2015).
- [2] Waldemar Bauer et al. “Development of in-situ Space Debris Detector”. In: *Advances in Space Research* 54.9 (2014), pp. 1858–1869. DOI: [10.1016/j.asr.2014.07.035](https://doi.org/10.1016/j.asr.2014.07.035).
- [3] Grigory Beskin et al. “From TORTORA to MegaTORTORA—Results and Prospects of Search for Fast Optical Transients”. In: *Advances in Astronomy* 2010 (2010). DOI: [10.1155/2010/171569](https://doi.org/10.1155/2010/171569).
- [4] Christopher R. Boshuizen et al. “Results from the Planet Labs Flock Constellation”. In: AIAA Conference on Small Satellites, Logan, UT, 2014.
- [5] Edward P. Chatters and Brian J. Crothers. “Space Surveillance Network”. In: *Air University Space Primer*. US Air Force, 2009, Ch.19. Chap. 19, pp. 249–258.
- [6] E.L. Christiansen, J.L. Hyde, and R.P. Bernhard. “Space Shuttle debris and meteoroid impacts”. In: *Advances in Space Research* 34.5 (2004), pp. 1097–1103. DOI: [10.1016/j.asr.2003.12.008](https://doi.org/10.1016/j.asr.2003.12.008).
- [7] Ryan D. Coder and Marcus J. Holzinger. “Multi-Objective Design of Optical Systems for Space Situational Awareness”. In: *Preprint submitted to Acta Astronautica* (2015).
- [8] T. A. Ely, W. A. Crossley, and E. A. Williams. “Satellite Constellation Design for Zonal Coverage Using Genetic Algorithms”. In: *Journal of the Astronautical Sciences* 47.3 and 4 (1999), pp. 207–228.
- [9] Matthew P. Ferringer et al. “Pareto-hypervolumes for the Reconfiguration of Satellite Constellations”. In: AIAA/AAS Astrodynamics Specialist Conference and Exhibit, Honolulu, HI, 2008. DOI: [10.2514/6.2008-6611](https://doi.org/10.2514/6.2008-6611).
- [10] W. Flury et al. “Searching for Small Debris in the Geostationary Ring”. In: *ESA Bulletin* 104 (2000).
- [11] J. L. Foster, J. R. Benbrook, and E. G. Stansbery. “Detection of small radar cross-section orbital debris with the Haystack radar”. In: *Space Debris*. Ed. by L. Anselmo. Vol. 35. Advances in Space Research. Kidlington: Pergamon Press Ltd, 2005, pp. 1210–1213. ISBN: 0273-1177. DOI: [10.1016/j.asr.2005.05.041](https://doi.org/10.1016/j.asr.2005.05.041).
- [12] Eric Frayssinhes. “Investigating new satellite constellation geometries with genetic algorithms”. In: AIAA/AAS Astrodynamics Specialists Conference, San Diego, CA, 1996, pp. 582–586.
- [13] X. J. Fu, G. M. Liu, and M. G. Gao. “Overview of orbital debris detection using spaceborne radar”. In: *Icica 2008: 3rd Ieee Conference on Industrial Electronics and Applications, Proceedings, Vols 1-3*. New York: IEEE, 2008, pp. 1071–1074. ISBN: 978-1-4244-1718-6.

- [14] Michael E. Gaposchkin, Curt von Braun, and Jayant Sharma. “Space-Based Space Surveillance with the Space-Based Visible”. In: *Journal of Guidance Control and Dynamics* 23.1 (2000), pp. 148–152. DOI: [10.2514/2.4502](https://doi.org/10.2514/2.4502).
- [15] George Gleghorn. “Orbital debris: A Technical assessment”. In: Committee on Space Debris, National Research Council, National Academy Press, 1995. ISBN: 0-309-58716-6.
- [16] Alan A. Grometstein. “MIT Lincoln Laboratory Technology in Support of National Security”. In: Lexington, MA: Lincoln Laboratory, 2011. ISBN: 978-0-615-42880-2.
- [17] Mike Gruntman. “Passive optical detection of submillimeter and millimeter size space debris in low Earth orbit”. In: *Acta Astronautica* 105.1 (2014), pp. 156–170. DOI: [10.1016/j.actaastro.2014.08.022](https://doi.org/10.1016/j.actaastro.2014.08.022).
- [18] Robert F. Hale. “United States Department Of Defense Fiscal Year 2016 Budget Request”. In: Department of Defense, Office of the Under Secretary of Defense, Chief Financial Officer, 2015.
- [19] Daniel J. Heimerdinger. “Orbital Debris and Associated Space Flight Risks”. In: *Reliability and Maintainability Symposium*. Alexandria, VA, IEEE, 2005. DOI: [10.1109/RAMS.2005.1408413](https://doi.org/10.1109/RAMS.2005.1408413).
- [20] Marcus J. Holzinger et al. “Photometric Attitude Estimation for Agile Space Objects with Shape Uncertainty”. In: *Journal of Guidance, Control, and Dynamics* 37.3 (2014). DOI: [10.2514/1.58002](https://doi.org/10.2514/1.58002).
- [21] Maryann Hutchison, Kristen M. Kolarik, and Jeffrey Water. “Joint Space Operations Center (JSpOC) Mission System (JMS) Common Data Model: Foundation for Interoperable Data Sharing for Space Situational Awareness”. In: The Aerospace Corporation Ground System Architectures Workshop Los Angeles CA, 2013.
- [22] Shirley Kan. *China’s Anti-Satellite Weapon Test*. Report. Congressional Research Service, Library of Congress order code RS22652, 2007.
- [23] T. S. Kelso. “Analysis of the Iridium 33-Cosmos 2251 collision”. In: *Astrodynamics* 135(1-3) (2010), pp. 1099–1112. ISSN: 1081-6003 978-0-87703-557-2.
- [24] Donald J. Kessler and Burton G. Cour-Palais. “Collision Frequency of Artificial Satellites: The Creation of a Debris Belt”. In: *Journal of Geophysical Research* 83.A6 (1978), pp. 2637–2646. DOI: [10.1029/JA083iA06p02637](https://doi.org/10.1029/JA083iA06p02637).
- [25] Huseyin Kiremitci. “Satellite Constellation Optimization for Turkish armed forces”. In: Naval Postgraduate School, Masters Thesis, 2013.
- [26] Wiley J. Larson and James R. Wertz. “Space Mission Analysis and Design”. In: 3rd edition, Space Technology Library. Microcosm, Ch. 19, 1999. ISBN: 978-1881883104.
- [27] Katarzyna Malek et al. “General overview of the ‘Pi of the Sky’ system”. In: *Photonics Applications in Astronomy, Communications, Industry, and High-Energy Physics Experiments*. Vol. 7502. 2009. DOI: [10.1117/12.837741](https://doi.org/10.1117/12.837741).

- [28] J. C. Mandeville, C. R. Maag, and C. Durin. “In-situ detection of micrometeoroids and orbital debris: The PIE experiment on MIR”. In: *Sample Return Missions to Small Bodies*. Ed. by T. Mukai and B. C. Clark. Vol. 25. Advances in Space Research-Series. Oxford: Pergamon Press Ltd, 2000, pp. 329–334. ISBN: 0273-1177. DOI: [10.1016/s0273-1177\(99\)00949-7](https://doi.org/10.1016/s0273-1177(99)00949-7).
- [29] P. Maskell and L. Oram. “Sapphire: Canada’s Answer to Space-Based Surveillance of Orbital Objects”. In: AMOS Technologies Conference, Maui, HI, 2008.
- [30] William J. Mason, Victoria Coverstone-Carroll, and John W. Hartmann. “Optimal Earth Orbiting Satellite Constellations Via a Pareto Genetic Algorithm”. In: 1998. DOI: [10.2514/6.1998-4381](https://doi.org/10.2514/6.1998-4381).
- [31] D. S. McKnight and F. R. Di Pentino. “New insights on the orbital debris collision hazard at GEO”. In: *Acta Astronautica* 85 (2013), pp. 73–82. ISSN: 0094-5765. DOI: [10.1016/j.actaastro.2012.12.006](https://doi.org/10.1016/j.actaastro.2012.12.006).
- [32] D. Monet et al. “Rapid Cadence Collections with the Space Surveillance Telescope”. In: US Naval Observatory Flagstaff Station, 2012.
- [33] Michael Morton and Timothy Roberts. “Joint Space Operations Center (JSpOC) Mission System (JMS)”. In: *AMOS Technologies Conference, Maui, HI*. 2011.
- [34] Craig Murray. “China Missile Launch May Have Tested Part of a New Anti-Satellite Capability”. In: US Congress, US-China Economic and Security Review Commission, 2013.
- [35] “National Space Policy of the United States of America”. In: Office of the President of the United States, Washington, D.C., 2010.
- [36] Ryan Nugent et al. “The CubeSat: The Picosatellite Standard for Research and Education”. In: *AIAA SPACE Conference and Exposition San Diego CA* (2008). DOI: [10.2514/6.2008-7734](https://doi.org/10.2514/6.2008-7734).
- [37] Tolulope E. O’Brien. “Space Situational Awareness Cubesat Concept of Operations”. In: Naval Postgraduate School, Masters Thesis, 2011.
- [38] D.L. Pollacco et al. “The WASP Project and the SuperWASP Cameras”. In: *Publications of the Astronomical Society of the Pacific* 118 (2006), pp. 1407–1418. DOI: [10.1086/508556](https://doi.org/10.1086/508556).
- [39] A. E. Potter. “Ground-based optical observations of orbital debris - a review”. In: ed. by W. Flury. Vol. 16. Advances in Space Research 11. Pergamon Press Ltd, 1995, pp. 35–45. ISBN: 0273-1177 0-08-042636-0. DOI: [10.1016/0273-1177\(95\)98751-9](https://doi.org/10.1016/0273-1177(95)98751-9).
- [40] “Report of the Scientific and Technical Subcommittee on its fifty-second session”. In: vol. 10(19). United Nations, Committee on the Peaceful Uses of Outer Space, 2015. ISBN: A/AC.105/1088.
- [41] Curtis M. Scaparotti. “Joint Publication 3-14, Space Operations”. In: US Department of Defense Joint Chiefs of Staff Washington D.C., 2013.

- [42] T. Schildknecht. *Optical Astrometry of Fast Moving Objects Using CCD Detectors*. Zurich, Switzerland: Institut fur Geodasie und Photogrammetrie, 1994.
- [43] Jayant Sharma et al. “Toward Operational Space-Based Space Surveillance”. In: *Lincoln Laboratory Journal* 13.2 (2002), pp. 309–334.
- [44] James R. Shell. “Optimizing orbital debris monitoring with optical telescopes”. In: AMOS Technologies Conference, Maui, HI, 2010.
- [45] Debi Shoots. “International space station performs fourth and fifth debris avoidance maneuvers of 2014”. In: vol. 19(1) *Orbital Debris Quarterly*. NASA Orbital Debris Program Office, 2015.
- [46] Debi Shoots. “Update on 3 Major Debris Clouds”. In: vol. 14(2) *Orbital Debris Quarterly*. NASA Orbital Debris Program Program Office, 2010.
- [47] Lance M. Simms et al. “Optical Payload for the STARE Mission”. In: SPIE Defense and Security Conference, Orlando, FL, 2011.
- [48] Lance M. Simms et al. “Space-based telescopes for actionable refinement of ephemeris pathfinder mission”. In: *Optical Engineering* 51.1 (2012), p. 011004. DOI: [10.1117/1.OE.51.1.011004](https://doi.org/10.1117/1.OE.51.1.011004).
- [49] Adam Snow et al. “Optimization of CubeSat Constellations for Uncued Electrooptical Space Object Detection and Tracking”. In: *AIAA Journal of Spacecraft and Rockets* 53 (3 2016). DOI: [10.2514/1.A33386](https://doi.org/10.2514/1.A33386).
- [50] Eugene G Stansbery et al. *NASA Orbital Debris Engineering Model ORDEM 3.0-Users Guide*. Tech. rep. NASA Johnson Space Center, Houston, TX, 2012.
- [51] “Technology Horizons”. In: vol. 1. Office of the US Air Force Chief Scientist, Library of Congress, 2011. ISBN: AF/ST-TR-10-01-PR.
- [52] Russell F. Teehan. “Responsive Space Situation Awareness in 2020”. In: US Air Force, Maxwell Air Force Base, 2007.
- [53] T. W. Thompson et al. “Radar detection of centimeter-sized orbital debris - preliminary arecibo observations at 12.5-cm wavelength”. In: *Geophysical Research Letters* 19.3 (1992), pp. 257–259. ISSN: 0094-8276. DOI: [10.1029/91g102772](https://doi.org/10.1029/91g102772).
- [54] Ting Wang. “Analysis of Debris from the Collision of the Cosmos 2251 and the Iridium 33 Satellites”. In: *Science and Global Security* 18.2 (2010), pp. 87–118. DOI: [10.1080/08929882.2010.493078](https://doi.org/10.1080/08929882.2010.493078).
- [55] Roman Wawrzaszek et al. “Possible use of the ‘Pi of the Sky’ system in a Space Situational Awareness program”. In: *Photonics Applications in Astronomy, Communications, Industry, and High-Energy Physics Experiments*. Vol. 7502. 2009.
- [56] David O. Whitlock. “History of on-orbit satellite fragmentations”. In: 13th edition, Lyndon B. Johnson Space Center, 2004. ISBN: JSC 62530.